HHS Public Access

Author manuscript

Nat Neurosci. Author manuscript; available in PMC 2021 April 23.

Published in final edited form as:

Nat Neurosci. 2020 November ; 23(11): 1352–1364. doi:10.1038/s41593-020-00724-1.

Activated microglia cause metabolic disruptions in developmental cortical interneuron that persist in schizophrenia-patient-derived interneurons

Gun-Hoo Park[a,#], **Haneul Noh**[a,b,#], **Zhicheng Shao**[b], **Peiyan Ni**[a,b], **Yiren Qin**[a], **Dongxin Liu**[a], **Cameron P. Beaudreault**[a], **Joy S. Park**[a], **Chiderah P. Abani**[a], **James M. Park**[a], **Derek T. Le**[a], **Sasha Z. Gonzalez**[a], **Youxin Guan**[a], **Bruce M. Cohen**[b], **Donna L. McPhie**[b], **Joseph T. Coyle, M.D.**[b], **Thomas A. Lanz**[c], **Hualin S Xi**[d], **Changhong Yin**[e], **Weihua Huang**[e], **Hae-Young Kim**[f], **Sangmi Chung**[a,b]

[a.]Department of Cell biology and Anatomy, New York Medical College, Valhalla, NY 01595, USA

[b.]Department of Psychiatry, McLean Hospital/Harvard Medical School, Belmont, MA 02478, USA

[c.]Internal Medicine Research Unit, Pfizer Inc., Cambridge, Massachusetts, USA

[d.]Computational Sciences, Pfizer Inc., Cambridge, Massachusetts, USA

[e.]Department of Pathology, New York Medical College, Valhalla, NY 01595, USA

[f.]Department of Public Health, New York Medical College, Valhalla, New York, USA

Abstract

The mechanisms by which prenatal immune activation increase risk for neuropsychiatric disorders are unclear. Here, we generated developmental cortical interneurons (cINs), known to be affected in schizophrenia (SCZ) when matured, from induced pluripotent stem cells (iPSCs) from healthy controls (HC) and SCZ patients, and cocultured them with or without activated microglia. Coculture with activated microglia disturbed metabolic pathways, as indicated by unbiased transcriptome analysis, and impaired mitochondrial function, arborization, synapse formation and

Correspondence and Lead Contact: Sangmi Chung, Ph.D., Address: BSB 220, New York Medical College, 15 Dana Rd, Valhalla, NY 10595, Tel: 914-594-4708, Fax: 914-594-4669, schung8@nymc.edu.

[#]equal contributors

Authors contributions:

G.-H.P, H.N., Z.S., P.N., Y.Q., B.M.C., J.T.C. and S.C. designed the experiments. G.-H.P, H.N., Z.S., P.N., Y.Q. and D.L differentiated cortical interneurons and analyzed them by qPCR and immunocytochemistry. G.-H.P., H.N. and P.N. analyzed oxidative phosphorylation of cortical interneurons using a Seahorse Analyzer. G.-H.P, H.N., C.P.B., J.S.P., C.P.A., J.M.P., D.T.L., S.Z.G. and Y.G. performed arborization analysis. G.-H.P, H.N., C.P.A. and J.M.P. analyzed inhibitory synapses in cIN organoids. G.-H.P. performed and analyzed synaptic GABA release analysis. B.M.C. and D.L.M., provided patient cell lines and reviewed data interpretation and manuscript contents. T.A.L., H.S.X., C.Y. and W.H. did RNA-seq analysis. H.-Y.K. performed statistical analysis. G.-H.P. and S.C. wrote the manuscript. S.C. supported this study financially.

Accession codes

The RNA-seq data were deposited at the GEO < https://www.ncbi.nlm.nih.gov/geo/> and the accession numbers are GSE118313, GSE132689 and GSE152438.

Disclosure of Potential Conflicts of interest

Thomas A. Lanz and Hualin S. Xi were employees of Pfizer, Inc at the time this work was performed. Joseph T. Coyle reports holding a patent on the use of D-serine to treat serious mental disorders that is owned by Massachusetts General Hospital and consulting with Concert Pharm.

synaptic GABA release. Deficits in mitochondrial function and arborization were reversed by Alpha Lipoic Acid/Acetyl-L-Carnitine (ALA/ALC) treatments that boost mitochondrial function. Notably, activated microglia-conditioned medium altered metabolism in cINs and HC-derived iPSCs but not in SCZ-patient-derived iPSCs or in glutamatergic neurons. After removal of activated microglia-conditioned medium, SCZ cINs but not HC cINs showed prolonged metabolic deficits, suggesting an interaction between SCZ genetic backgrounds and environmental risk factors.

Introduction

Epidemiological studies have frequently associated maternal infection with later development of neuropsychiatric disorders, including schizophrenia (SCZ) and autism spectrum disorders (ASD), in their offspring [1,2]. In fact, not only maternal infection, but other environmental factors that increase maternal immune responses, such as autoimmune disorders, allergies, asthma, acute stress and pollutants, have all been linked to increased risk of ASD and SZ [3,4], suggesting a key role of prenatal immune activation, even in the absence of direct pathogens, in disturbing normal neurodevelopment with long-lasting consequences later in life. Shortly after maternal immune activation, induction of multiple cytokines in the fetal brain are observed in rodent models [4] and activated microglia were observed in fetal sheep brains [5–7]. However, the mechanisms whereby the activation of the immune system during gestation can bring about such long-lasting consequences of disease susceptibility are not well understood.

One of the most consistently affected neuronal types in the brains of individuals with SCZ is GABAergic cINs, especially those expressing parvalbumin (*PVALB*) or somatostatin (*SST*)[8,9], which are derived from the medial ganglionic eminence (MGE) during early development. Altered cIN neurotransmission in SCZ may account for abnormalities in gamma oscillation, which are associated with cognitive impairments in SCZ patients [10]. Consistent with this hypothesis, in one study, pharmacological activation of $GABA_A$ receptors restored gamma band activity in people with SCZ, accompanied by some degree of improved cognitive function [11]. Furthermore, preclinical animal models of maternal immune activation display “SCZ-like” cIN disturbances, including abnormalities in cIN-specific gene expression patterns and impaired inhibitory neurotransmission[1], thus providing a model system to study the interaction between environmental risk factors and the SCZ genetic background.

Much of our understanding on the impact of prenatal immune activation during neurodevelopment comes from preclinical animal models, especially in rodents, that have produced a wealth of information potentially relevant to human disorders[12]. However, inherent differences between rodents and humans limit the usefulness of using rodents when it comes to studying uniquely human processes and/or uniquely human disorders such as SCZ. For example, the interaction between SCZ genetic burden and environmental risk cannot be adequately studied in rodent models that cannot recapitulate the hundreds of SCZ genetic risk loci that are mostly in non-coding regions, which are not well conserved

between humans and rodents. The lack of informative human fetal tissues has long hampered understanding of the pathogenesis of SCZ.

Based on the high heritability of SCZ [13], iPSC technology [14] can be used to generate disease-relevant tissues with the same genetic composition as the patient's neurons and to study molecular and cellular abnormalities occurring during early development[15]. To succeed requires the ability to generate well-defined and highly enriched populations of disease-relevant cell types consistently from iPSCs. Many iPSC-derived neurons used in prior SCZ studies have been mixed populations of different neuronal subtypes [16], often containing varying proportions of the subtypes from batch to batch. Such heterogeneity can result in variability of culture composition, increasing the risk of misleading differences, and an inability to identify abnormalities of specific processes in specific cell types. This issue was also observed in a recent large-scale postmortem transcriptome analysis that showed that cell composition differences among individuals was the most substantial contributor to variation in individual bulk RNA-seq [17], stressing the importance of using highly enriched specific cell populations to clearly identify disease-dependent changes free of cell composition confounders. We have successfully resolved this issue by developing an efficient method of generating a highly enriched population of MGE-derived cINs from human pluripotent stem cells (hPSCs) and extensively confirming their authenticity and functionality *in vitro* and *in vivo* in our previous studies[18,19]. In our previous study, these highly enriched populations of developmental cINs derived from iPSCs from subjects with SCZ allowed us to effectively analyze transcriptome changes, revealing metabolic dysfunction as a major pathway disturbance associated with assumed SCZ genomic burden in these neurons [20].

To identify how prenatal immune activation affects neurodevelopment, especially for developmental cINs, we cocultured highly enriched populations of cINs with activated microglia, performed unbiased genome-wide transcriptome analyses and identified deficits in metabolic pathways as one of the major abnormalities in developing cINs under this condition. Disruption in metabolic pathway gene expression was associated with mitochondrial hypofunction in developing cINs, accompanied by compromised energy-dependent neuronal processes such as arborization, synapse formation and synaptic GABA release. Mitochondrial hypofunction and arborization deficits were reversed by treating the cells with ALA/ALC, a chemical combination shown to boost mitochondrial function[21]. The metabolic dysfunction effect of activated microglia co-culture was not mimicked by addition of IL17 [22,23], indicating that IL17 is not the mediator of its metabolic impact on cINs. Long after the removal of inflammatory stressors, only the SCZ cINs, but not the HC cINs, displayed disrupted metabolic pathways, suggesting that an SCZ genetic background interacts with an inflammatory environment (activated microglia). This study provides a platform to dissect and model cellular and molecular changes intrinsic to specific disease-relevant neural populations during development and may help to identify novel therapeutic targets to better treat/prevent SCZ, including cIN-associated symptoms like cognitive deficits, which are not adequately responsive to current anti-psychotic treatments.

Results

Co-culture with activated microglia results in metabolic pathway dysregulation in developmental cINs

Infection in the pregnant mother is frequently associated with later risk for neuropsychiatric disorders in offspring, but the mechanism by which infection or inflammation, in general, alters neurodevelopmental processes is not clear. To identify the mechanism of neurodevelopmental abnormalities of cINs caused by an inflammatory environment in fetal brains [4–7], we generated a highly enriched population of cINs from 4 HC vs 4 SCZ iPSC lines (Extended Data 1A) according to our previously described protocol [18,24] (Extended Data 1B). Extensive immunocytochemistry and cell counting analyses showed high homogeneity of developmental cIN generation (Extended Data 1D–E). For co-culture of developmental cINs with inflammatory cytokine-releasing microglia (Fig. 1A), we generated activated microglia by treating microglial BV2 cells with 1ug/ml LPS and 1ug/ml polyI-C overnight in a tissue culture insert. Treated microglia showed significant increases in the expression of various inflammation-associated molecules, such as *IL-1β*, *IL-6*, *NOS2* (also known as *iNOS*) and *TNF* (also known as *TNFα*) (Fig. 1B and Extended Data 1C). Developmental cINs with or without activated microglia co-culture were subjected to RNA-seq analysis (Extended Data 2A–B and Supplementary Table 1). Consistent with immunocytochemistry analysis, generated cINs showed very low expression of non-relevant markers, such as the pluripotent stem cell marker *NANOG*, the astroglial marker *GFAP*, the oligodendrocyte marker *MBP*, the glutamatergic neuronal progenitor marker *PAX6*, the glutamatergic neuronal marker *SLC17A7* (also known as *VGLUT1*), the cholinergic neuronal marker *CHAT*, the dopaminergic neuronal marker *TH*, or the serotonergic neuronal marker *TPH1*, but very high expression of relevant markers such as neuronal markers *MAP2* and *DCX*, MGE progenitor markers *NKX2-1*, and the cIN markers *SLC32A1* (also known as *VGAT*), *GAD1*, *FOXG1* and *LHX6*, regardless of their co-culture status with activated microglia (Fig. 1C and Extended Data 2C). However, the expression of inflammatory response genes *NF-κBIZ*, *TNFRSF12A*, *TNFAIP3* and *NFATC2* was significantly increased in developmental cINs co-cultured with activated microglia when compared to the control conditions by RNA-seq (Fig. 1D). These findings were confirmed by quantitative PCR (qPCR) analysis (Extended Data 2D). Some of these inflammatory markers were also significantly upregulated in the recent large-scale PsychENCODE postmortem SCZ RNA-seq analysis [25] (Extended Data 2E). These results demonstrate that co-culture with activated microglia induces an inflammatory response in developmental cINs, successfully modeling fetal brain inflammatory environment in a well-defined system.

To understand the changes induced by co-culture with activated microglia on developmental cINs, we performed pathway analysis of the differentially expressed (DE) genes (Supplementary Table 2). Among the six top DE gene pathways, GO:0019222 (regulation of metabolic process) encompasses the majority of the DE genes and the majority of the other top pathway genes (Fig. 1E and Supplementary Table 3). However, the expected inflammatory response pathways did not show up as highly significant pathways, though a number of inflammatory response genes were upregulated (Fig. 1D and Extended Data 2D). This was an interesting observation in light of our recent results where we showed that

developmental cINs from subjects with SCZ exhibited metabolic dysfunction [20], suggesting a convergence of pathways affected by presumed SCZ genomic burden and pathways affected by an environmental risk factor for SCZ (inflammation). Among the genes shared among top DE gene pathways (Supplementary Table 3), *CCN2* (also known as *CTGF*) and *THBS1* showed the greatest fold changes in developmental cINs under co-culture with activated microglia (Fig. 1F), which was confirmed by qPCR analysis (Fig. 1G). Both *CTGF* and *THBS1* were shown to be activated in inflammatory conditions, in various tissues including fibroblast [26] , brain [27] and skin [28], suggesting their role in inflammatory responses. *THBS1* was also upregulated in the recent large-scale PsychENCODE postmortem SCZ RNA-seq analysis [25] (Extended Data 2F). In addition, *CTGF* and *THBS1* were shown to negatively affect metabolism in cancer cells [29] and adipose tissues[30], respectively. To further test and confirm the observed molecular changes, we differentiated 12 more iPSC lines (6 HC and 6 SCZ lines) to developmental cINs, and subjected these lines to co-culture with activated microglia. As in the original cohort, we observed a significant increase in *CTGF* and *THBS1* expression levels in developmental cINs co-cultured with activated microglia (Fig. 1H and Extended Data 3A–B) in this cohort (Extended Data 4A–B) without significant changes in neuronal phenotype as analyzed by the expression of *GAD1* and *SOX6* (Extended Data 4C). These results point to metabolic pathways as the major target in developmental cINs co-cultured with activated microglia, most prominently accompanied by upregulation of *CTGF* and *THBS1.*

Altered metabolic gene expression results in a deficit in mitochondrial function, arborization, and synapse formation in developmental cINs cultured in activated microglia-conditioned media

Next, we addressed whether the above changes in metabolic gene expression have functional consequences. Thus, we analyzed mitochondrial function of developmental cINs with or without activated microglia-conditioned media using a Seahorse Analyzer (Extended Data 5A–B). There was a significant decrease in basal respiration, maximum respiration and ATP production, but no changes in glycolysis, for the developmental cINs that were incubated with activated microglia-conditioned media (Fig. 2A and Extended Data 5D), suggesting mitochondrial dysfunction is not compensated by increased glycolysis under these conditions. Since *CTGF* and *THBS1* were the major metabolic regulators altered by co-culture with activated microglia in developmental cINs, we determined whether overexpression of *CTGF* and *THBS1* (Extended Data 5C) could recapitulate the metabolic dysfunction observed in these neurons. Indeed, basal respiration, maximum respiration and ATP production were all significantly decreased by overexpression (Fig. 2B and Extended Data 5E), demonstrating a role for these two induced genes in negatively regulating cIN metabolism. Furthermore, we examined the effect of siRNA-mediated knock down of *CTGF* and *THBS1* (Extended Data 5C) on developmental cINs cultured in activated microglia-conditioned media and observed siRNA treatment significantly increased basal respiration, maximum respiration and ATP production in these cells (Fig. 2C and Extended Data 5F), reversing the deficits observed under this condition. These results point to a causal role for *CTGF* and *THBS1* in the metabolic dysfunction of developmental cINs cultured in activated microglia-conditioned media.

Since in our previous study, we observed metabolic dysfunction in SCZ developmental cINs was associated with arborization deficits [20], we examined whether the metabolic dysfunction described above can lead to arborization deficits in developmental cINs (Fig. 2D). Developmental cINs cultured in activated microglia-conditioned media exhibited arborization deficits with reduced total neurite lengths and branch numbers (Fig. 2E–F, Extended Data 6A and Extended Data 7E). As in our previous study [20], these arborization deficits could be reversed by treating the cells with ALA/ALC, a chemical combination shown to boost mitochondrial function (Extended Data 6B). In addition, we analyzed whether synapse formation, another energy-dependent cIN function [31–33], may have been compromised in developmental cINs cultured in activated microglia-conditioned media (Fig. 2G). We observed a significant decrease in synapse formation in developmental cIN organoids cultured in activated microglia-conditioned media compared to the control cIN organoids (Fig. 2H and Extended Data 6C–D), suggesting that compromised metabolic function in cINs during development may hinder proper circuit formation.

SCZ cINs but not HC cINs show prolonged metabolic dysregulation after the removal of inflammatory stressors

To explore whether the response to co-culture with activated microglia differed between developmental cINs from SCZ patients and those from HCs, we analyzed DE genes in HC cINs and SCZ cINs separately. As shown in Fig. 3A and Supplementary Tables 4–5, there were some DE genes shared by HC cINs and SCZ cINs, but the majority of DE genes did not overlap between two DE gene sets. Next, we examined HC-specific DE genes and SCZ-specific DE genes for enriched pathways. Interestingly, although the individual genes that were dysregulated by co-culture with activated microglia specifically in HC cINs and specifically in SCZ cINs were different, both of these specific DE genes showed enrichment of metabolic pathways (Fig. 3B). Furthermore, *CTGF* and *THBS1* were upregulated both in HC cINs and SCZ cINs co-cultured with activated microglia (Fig. 3C, Extended Data 3A–B and Extended Data 7A). In line with pathway analysis, Seahorse analyses in HC cINs and SCZ cINs showed that mitochondrial function is compromised both in HC cINs and SCZ cINs cultured in activated microglia-conditioned media (Fig. 3D and Extended Data 7B), each accompanied by compromised arborization (Fig. 3E and Extended Data 6A).

Since many aspects of the prenatal immune activation have been shown to be mediated by IL17 [22,23], we examined whether IL17 treatment might result in a dysfunction in metabolic pathways similar to that observed with the activated microglia treatment in developmental cINs (Fig. 4A). RNA-seq results showed that IL17 treatment induced significant increases on the expression of various inflammation genes, *IL2RA*, *TNFRSF1B*, *IRF5* and *IRAK3* (Fig. 4B). However, unlike co-culture with activated microglia, IL17 treatment was not associated with disruption of metabolic pathways either in HC cINs nor in SCZ cINs (Fig. 4C–D and Supplementary Tables 6–7). Comparisons of DE gene lists between co-culture with activated microglia and IL17 treatment revealed only a few overlapping genes either in HC cINs or SCZ cINs (Fig. 4E–F), though both conditions induced the expression of inflammatory genes (Fig. 1D, Fig. 4B and Extended Data 2D). This result suggests specificity of cIN response to different inflammatory stimuli.

Prenatal immune activation can cause long-lasting changes in developing brains that remain long after the termination of the initial inflammatory stressor, and this is thought to increase the risk of various psychiatric disorders. We therefore assessed whether changes induced in cINs by co-culture with activated microglia persist after the removal of this inflammatory stressor. Developmental cINs were co-cultured with activated microglia, followed by washing and incubation in normal media for 7 days, then assessed for gene expression changes in this delayed phase by RNA-seq (Fig. 5A), followed by enriched pathway analysis of HC-specific DE genes and SCZ-specific DE genes. We found that SCZ cINs exhibited persistent disruption of metabolic pathways, with most of the significantly affected pathways associated with the "cellular metabolic process" parent GO term; this was not seen in HC cINs at this time point (Fig. 5B–E and Supplementary Tables 8–9), which instead had DE genes associated with parent GO terms like "regulation of hormone levels" and "cell activation". This indicates SCZ cIN-specific persistent responses long after the removal of the activated microglia. Significantly altered metabolic genes in SCZ cINs in the delayed phase were not altered in HC cINs under the same conditions (Fig. 5F). Among the significantly altered metabolic genes in SCZ cINs, *KLF5* showed the most prominent fold changes (Fig. 5F), whereas this gene was not altered in HC cINs, a result which was confirmed by qPCR analysis (Fig. 5G and Extended Data 3C). *KLF5* has been shown to activate a number of metabolic genes in various tissues such as skeletal muscle cells [34] and cardiac myocytes [35]. We also analyzed the expression change of *KLF5* in the replication cohort and again observed significant downregulation of *KLF5* in SCZ cINs but not in HC cINs during the delayed phase (Fig. 5H, Extended Data 3D and Extended Data 7C). In line with the disrupted metabolic gene expression in SCZ cINs long after removal of the activated microglia, we observed significant deficits in maximum respiration, basal respiration and ATP production in SCZ cINs but not in HC cINs in this delayed phase (Fig. 5I, Extended Data 5G–H and Extended Data 7D). This result suggests an interaction between assumed SCZ genomic burden and environmental risk factors, where the response to environmental risk factors depends on the genetic 'SCZ risk' background, which we here modeled by using a highly enriched population of developmental cINs generated from patient iPSCs and HC iPSCs.

Human cINs but not human glutamatergic neurons nor SCZ iPSCs show metabolic responses when cultured in activated microglia-conditioned media

We further confirmed cINs' intrinsic inflammatory response using HMC3, microglia of human fetal origin [36] (Fig. 6A–B). Upon activation with 1ug/ml LPS and 1ug/ml polyI-C overnight, HMC3 released significantly higher levels of IL6, assayed by human IL6-specific ELISA kit (R&D Systems) (Fig. 6C). Developmental cINs cultured in activated HMC3-conditioned media showed increased expression of inflammatory genes including *NFκBIZ*, *TNFRSF12A* and *TNFAIP3* (Extended Data 8A), showing that activated HMC3-conditioned media induces an inflammatory response in cINs. In addition, activated HMC3-conditioned media induced *CTGF* and *THBS1* expression in both HC cINs and SCZ cINs (Extended Data 8B), consistent with the result from the BV2 co-culture system (Fig. 3C and Extended Data 3A–B). Induction of *CTGF* and *THBS1* expression by activated HMC3-conditioned media was accompanied by compromised mitochondrial function in both HC cINs and SCZ cINs (Fig. 6D, Extended Data 9A–B and Extended Data 9E). Considering the fact that

culture in activated microglia-conditioned media compromised energy-dependent neuronal function, including arborization and synapse formation in cINs (Fig. 2D–H), we tested whether activated microglia-conditioned media resulted in compromised synaptic GABA release. Indeed, exposure to activated HMC3-conditioned media compromised action potential firing-dependent synaptic GABA release in both HC cINS and SCZ cINs; GABA release was restored by addition of ALA/ALC, a chemical combination shown to boost mitochondrial function (Fig. 6E and Extended Data 9G), suggesting that metabolic deficits were responsible for the observed compromised synaptic release. One week after the removal of HMC3-conditioned media, HC cINs no longer showed metabolic dysfunction, whereas SCZ cINs persistently showed compromised metabolism (Fig. 6F, Extended Data 9C–D and Extended Data 9F), accompanied by down-regulation of *KLF5* (Extended Data 8C). As expected from compromised metabolism in SCZ cINs but not in HC cINs in this delayed phase, action potential firing-dependent synaptic GABA release was compromised in SCZ cINs but not in HC cINs (Fig. 6G and Extended Data 9H). ALA/ALC treatment restored the synaptic release deficits in SCZ cINs in the delayed phase that resulted from earlier exposure to activated HMC3-conditioned media, without affecting GABA release in HC cINs (Fig. 6G).

Having confirmed that metabolic deficits were induced by exposure to multiple microglial systems, we then tested whether compromised metabolism by activated microglia-conditioned media was specific to developmental cINs or also observed in glutamatergic neurons. Thus, we generated developmental glutamatergic neuron-enriched populations from human iPSCs obtained from HCs and SCZ patients (Fig. 7A–B). When cultured in activated HMC3-conditioned media, neither HC glutamatergic neurons nor SCZ glutamatergic neurons showed any metabolic deficits, and neither showed *CTGF* and *THBS1* induction (Fig. 7C–D and Extended Data 10A–C). We also tested the response of iPSCs, from which developmental cINs and glutamatergic neurons were derived. HC iPSCs, but not SCZ iPSCs, showed a significant increase in mitochondrial function, when cultured in activated HMC3-conditioned media (Fig. 7E). These result shows that the decreased metabolic function under inflammation is not a general phenomenon observed in all cell types.

Discussion

In this study, employing unbiased genome-wide analysis of transcriptome changes in highly enriched populations of developing SCZ cINs, we observed compromised metabolic pathways as a major disturbance produced by co-culture with activated microglia, rather than the more expected immune pathway disturbances [4]. Though we observed induction of inflammatory genes (Fig. 1D, Extended Data 2D and Extended Data 8A), ‘inflammatory response’ did not show up as the major pathway disturbance. Both HC and SCZ cINs exhibited metabolic dysfunction during the acute phase of co-culture with activated microglia, converging with the effect of the assumed SCZ genomic burden in these cells [20]. By contrast, after the removal of activated microglia, only the SCZ cINs, not the HC cINs, continue to show metabolic dysfunction, which could reflect an interaction between the genetic backgrounds of SCZ donors and the inflammatory environment provided by co-culture with activated microglia. One caveat is that we could not show whether observed

changes in SCZ cINs are permanent. However, we did demonstrate lasting impacts in SCZ cINs even when all inflammatory stimulation by activated microglia co-culture has been completely removed for some time and HC cINs are fully recovered. This difference in the long-term response to inflammation between HC and SCZ cINs seems consistent with the observation that not all humans with prenatal immune activation will go on to develop SCZ and contrasts with findings from rodent models of maternal immune activation, where generally all offspring exhibit pronounced behavioral abnormalities [37]. Thus, a highly enriched population of developmental cINs provides a platform to reliably investigate the molecular and cellular consequences of interactions between presumed SCZ genetic burden in SCZ donor genomes and the environment, which is not possible in human postmortem tissues.

Mitochondrial metabolism is critically involved in many aspects of neuronal functions, including synaptic transmission[38], Ca^{2+} signaling[39], generation of action potentials [40] and ion homeostasis[41], enabling these energy demanding processes. Thus, it is conceivable that hypofunction of mitochondria could result in suboptimal neuronal development and function[42]. In line with the notion of metabolic dysfunction playing a role in SCZ pathogenesis [40], mitochondrial abnormalities caused by haploinsufficiency of *Mrpl40* (one of the 22q11DS locus genes) resulted in SCZ-relevant behavioral deficits in mice [43]. A recent study reported restoration of mitochondrial function in a rat model of SCZ by transplanting healthy mitochondria, which resulted in reversal of SCZ-like behavioral deficits [44]. Moreover, *Cox10* deletion in parvalbumin^{+} cINs results in abnormal gamma oscillations in the prefrontal cortex (PFC) and hippocampus, accompanied by deficits in sensory motor gating and sociability [45]. More recently, *Txnrd2*-mediated mitochondrial dysfunction resulted in cortical under-connectivity, which was reversed by anti-oxidant treatment [46], similar to our observation of suboptimal connectivity in cINs due to compromised mitochondrial function. Furthermore, tangential migration of immature cINs, but not radially migrating pyramidal neurons, depends on oxidative phosphorylation during brain development [47], suggesting that developing cINs may be more vulnerable to the observed metabolic dysfunction than developing pyramidal neurons. Thus, it is plausible that metabolic dysfunction in cINs, caused by the interaction between SCZ genomic burden and environmental risk factors, could result in a cascade of circuit abnormalities in SCZ patients, including altered interneuron migration and abnormal gamma oscillations, in which cINs connectivity plays a critical role[10].

Among the most prominently affected genes under activated microglia co-culture were *THBS1* and *CTGF* during the acute phase and *KLF5* during the delayed phase. Overall, it seems that modest changes in expression of many genes, each of which might not impact the overall function of mitochondria much, collectively could contribute to the impaired mitochondrial function. This would be in line with the multigenic/multi-risk nature of SCZ pathogenesis. Interestingly, among the >300 Psychiatric Genomics Consortium (PGC2) putative SCZ risk loci genes, there were significant enrichments of metabolic/mitochondrial genes (total 22 genes, $p<0.05$ by hypergeometric test)[48], supporting the potential role of mitochondrial dysfunction in SCZ pathogenesis. We did not find much direct overlap in specific genes between our metabolic inflammation DE genes and these PGC2 loci genes, nor between previous metabolic SCZ cIN DE genes and PGC2 genes; this suggests that

converging pathways, rather than specific genes, may identify potential therapeutic targets. Moreover, the differing components of the metabolic gene pathways, among acute inflammation DE genes in HC, acute inflammation DE genes in SCZ and delayed inflammation DE genes in SCZ, resulted in similar downstream effects, further supporting the hypothesis that metabolic pathways rather than specific genes could be a useful therapeutic target to treat/prevent SCZ with its quite heterogeneous etiology. Specifically, we observed that the functional deficit induced by activated microglia-conditioned media in cINs was reversed by treatment with ALA/ALC, further strengthening the notion that reversing cIN metabolic deficits could serve as a novel type of therapeutic intervention to prevent or reduce cIN-related SCZ pathology. Notably, although the direction of the effects was consistent among different subject lines tested in this study, the basal expression level and the magnitude of effects could vary depending on the genetic background of each subject (Extended Data 3A–D), just as different individuals may respond to the same stimuli/treatment in diverse ways. This finding is consistent with the call for personalized medicine that considers patient-specific responses and underscores the importance of using multiple lines (subjects) with diverse genetic backgrounds to fully study the impact of environmental factors on human developmental neurons.

Highly enriched populations of developmental cINs co-cultured with activated microglia resulted in transcriptome changes in metabolic gene expression, with enduring metabolic changes in the SCZ cINs but not in the HC cINs. We used activated microglia co-cultured in tissue culture inserts, or activated microglia-conditioned media, without direct contact between microglia and cINs, to model the effects of elevated levels of inflammatory molecules in the fetal brain following maternal immune activation [2,28,49]. One caveat of this study is that the study did not include co-culture with resting microglia due to the significant release of cytokines even in the absence of activation *in vitro* (Fig. 6C and Extended Data 1C), and thus it cannot be ruled out that (some of) the observed effects may be due to the presence of microglia per se, rather than due to their activated state. Another caveat is that microglia *in vitro* have distinct morphology and characteristics compared to those *in vivo*[28]; nevertheless, microglia both *in vivo* and *in vitro* (including the microglial cell lines that we used) respond to pathogens and release various key inflammatory cytokines and chemokines [36,50]. The alterations in developmental cINs were manifest in the absence of other neuronal subtypes such as glutamatergic neurons that can affect the functionality of cINs, revealing what is intrinsic to these SCZ cINs. In addition, decreased neuronal metabolism with activated microglia co-culture was specific to cINs during this early phase of development, not observed in developmental glutamatergic neurons. Considering that adult maternal immune activation offspring show deficits both in cINs and glutamatergic neurons[12], deficits in glutamatergic neurons in these offspring may be mediated by non-intrinsic mechanisms secondarily from the deficits in other cell types in the developing brains or by cell-intrinsic yet non-metabolic mechanisms. For iPSCs from which cINs and glutamatergic neurons are derived, HC iPSCs but not SCZ iPSCs showed a significant increase in metabolism when cultured in activated microglia-conditioned media, showing the opposite direction of changes compared to cINs.

Prenatal immune activation could affect the brain developmental trajectory via multiple mechanisms, of which we are modeling one aspect: the impact of heightened inflammatory

cytokines on development of cINs. In the next phase of this study, it will be critical to analyze which specific cytokines are involved in the observed effects in human cINs. Our findings showed that the effects were unlikely to be mediated by IL17, since incubating the developmental cINs with IL-17 did not reproduce the effects of co-culture with activated microglia. Future studies will require systematic blocking of various cytokines alone or in combination to address this question.

The results of this study demonstrate the utility of studying homogeneous disease-relevant cell populations as a means to investigate aspects of SCZ pathogenesis, including gene by environment interactions. Some of the abnormalities observed, which may not be detected in mixed cell populations, could help provide novel potential therapeutic targets for SCZ.

Online Methods

Differentiation of iPSCs and microglia coculture

Generation of iPSCs were described in our previous publications [18,20]. Ten male SCZ patient samples with age from 21 - 51 years old as well as ten age and gender-matched healthy control samples were used in this study as summarized in Extended Data 1A and Extended Data 4A. Human fibroblasts were obtained from the laboratories of Dr. Bruce Cohen (McLean Hospital), Dr. Daniel Weinberger (Lieber Institute for Brain Development), and Dr. Judith Rapoport (National Institute of Mental Health). These study protocols were approved by the McLean Hospital/Partners Healthcare Institutional Review Board (IRB) and New York Medical College IRB. All procedures were performed in accordance with IRB's guidelines and all human samples were obtained with informed consents. We have complied with all relevant ethical regulations. All non-McLean cohorts of iPSCs have been deposited to the NRGR biorepository. McLean cohorts of iPSCs will be available upon approval from the McLean Hospital/Partners Healthcare IRB.

Thawed human iPSCs were maintained on Matrigel (BD, San Hose, CA) coated plates with Essential 8 (E8) media (Invitrogen, Carlsbad, CA). For differentiation, iPSCs were trypsinized and grown as floating spheres in low adherent flasks in KSR media (DMEM, 15 % knockout serum replacement, 2 mM L-glutamine and 10 μM β-mercaptoethanol (all from Invitrogen) from day 0 to day 14. For neuroectoderm induction, cells were treated with LDN193189 (100 nM, Stemgent, Cambridge, MA) from day 0 to day 14 and SB431542 (10 μM, Tocris Cookson, Ellisville, MO) from day 0 to day 7. For MGE phenotype induction, media was supplemented with IWP2 (5 μM, EMD Millipore, Billerica, MA) from day 0 to day 7 and SAG (0.1 μM, EMD Millipore) from d0 to d21. From day 14, cells were grown in N2AA media (DMEM-F12 with N2-supplement (1:200, Invitrogen) and 200 μM ascorbic acid (AA, Sigma, St. Louis, MO). FGF8 (100 ng/ml, Peprotech, Rocky Hill, NJ) was added from day 14 to day 21 to induce the MGE phenotype at the expense of the CGE phenotype [24]. N2AA media was supplemented with 10 ng/ml glial cell derived neurotrophic factor (GDNF, Peprotech) and 10 ng/ml brain derived neurotrophic factor (BDNF, Peprotech) from day 21. At day 45 of differentiation, cIN spheres were trypsinized in the presence of 0.1M trehalose (Sigma) and then plated on polyornithine (PLO; 15 mg/ml; Sigma)- and fibronectin (FN; 1 mg/ml; Sigma)-coated plates in B27GB media (DMEM-F12 media with B27 supplement (1:100, Invitrogen), 10 ng/ml GDNF and 10 ng/ml BDNF). Each "batch" in

each experiment is an independent *in vitro* differentiation of iPSCs, which are samples comparable to identical twins, having exactly the same genetic background, but are exposed to non-identical environments during development.

For Glutamatergic neuron differentiation, iPSCs were trypsinized and grown as floating spheres in low adherent flasks in Neuronal induction media (DMEM-F12 with 15 % knockout serum replacement, 1% MEM-NEAA, 100μM β-mercaptoethanol (all from Invitrogen),100nM LDN193189 (Stemgent), 10μM SB431542 (Tocris Cookson) and 2μM IWP2 (ApexBio)) from day 0 to day 10. From day 11, cells were grown in Neuronal differentiation media (DMEM-F12 with 0.25% N2, 0.5% MEM-NEAA, 50μM β-mercaptoethanol (all from Invitrogen) and N21 MAX (R&D systems), until the spheres were trypsinized in the presence of 0.1M trehalose (Sigma) and plated on PLO/FN-coated plates in B27GB media after 8 weeks' differentiation for analysis.

For coculture with activated microglia, microglial BV2 cells were plated in the tissue culture insert (12,700 Cells/cm^2) and treated with 1ug/ml LPS (Sigma) and 1ug/ml polyI-C (Sigma) overnight, followed by coculture with cINs for 2 hours, followed by harvest for RNA prep using Trizol (Invitrogen) immediately for acute phase or after a week's culture in B27GB media for delayed phase. In some case, activated microglia-conditioned media was used in place of co-culture. For collection of conditioned media, 70% confluent microglia were treated with 1ug/ml LPS (Sigma) and 1ug/ml polyI-C (Sigma) overnight, followed by collection of conditioned media. Collected media was filtered using a 0.2um syringe filter unit (Millipore), aliquoted and frozen immediately until use. Activation of BV2 microglia were confirmed by Mouse IL-1β DuoSet ELISA kit (R&D systems) according to the manufacturer's instructions. Human fetal microglia HMC3 was purchased from ATCC (ATCC® CRL-3304™) and maintained in DMEM media with 10% FBS. For conditioned media collection, 70% confluent HMC3 microglia were treated with 1ug/ml LPS (Sigma) and 1ug/ml polyI-C (Sigma) overnight, followed by collection of conditioned media. Collected conditioned media was filtered using a 0.2um syringe filter unit (Millipore), aliquoted and frozen immediately until use. Activation of microglial HMC3 were confirmed by IL-6 ELISA analysis using human IL-6 ELISA kit (R&D systems) according to the manufacturer's instructions. We used no microglia coculture as controls due to baseline cytokine release from cultured microglia, though activation further increases the inflammatory cytokine expression. For IL17 treatment, 100ng/ml human recombinant IL17 protein (Cat# 7955-IL-025/CF, R&D systems) was added to cIN culture for 24hours and cells were harvested for RNA preparation. The cell lines used for each experiment were summarized in Supplementary Table 10.

RNA purification and qPCR analysis

RNA samples were isolated using a TRIzol-reagent (Invitrogen) and 300ng of the total RNA was used for cDNA synthesis using the $Oligo(dT)_{12-18}$ primer (Gene Link, Hawthorne, NY), Recombinant RNAse Inhibitor (Takara, Japan), 0.5 mM dNTP mix (Thermo Scientific, Waltham, MA), 5 mM DTT (Invitrogen), RevertAid H minus RT (Thermo Scientific), and 5X Reaction Buffer (Thermo Scientific) in SimpliAmp™ Thermal Cycler (Applied Biosystems, Waltham, MA). The real time PCRs were performed using the QuantStudio 3

Real-Time PCR System (ThermoFisher), with 40 cycles of denaturation (95°C for 15sec), annealing (55°C for 30sec), and extension (72°C for 30sec). Primer sequences are listed in Supplementary Table 11.

RNA-seq analysis

For RNA-seq, RNA quality was examined by the 2100 Bioanalyzer or 4200 TapeStation (Agilent Technologies, Santa Clara, CA) and RNA concentration was determined using the Qubit Fluorometric Quantitation (Thermo Fisher, Waltham, MA). Stranded cDNA libraries were prepared using the TruSeq Stranded HT or LT mRNA kit (Illumina, San Diego, CA) in accordance with the manufacturer's protocol using the poly-adenylated RNA isolation. Sequencing of paired-end reads (75 bp × 2) was performed on the NextSeq 550 or 500 system. Raw sequence reads were de-multiplexed and trimmed for adapters by using the Illumina bcl2fastq conversion software (v2.19). Sequence reads of each sample were aligned to the human hg19 reference genome with GENCODE v19 transcriptome annotation using STAR (v.2.4.0) and gene expression level was quantified as RPKM values using featureCount (v.2.0.0), taking into account the strandness of the reads and all transcript variants of each gene in the GENCODE annotation; or pseudo-aligned to the human hg38 reference transcriptome and the gene transcript abundance was quantified by using Kallisto (v.0.46.1). Differential expression of genes and transcripts were achieved by using the Sleuth and/or DESeq2 (v.1.26.0) in R Studio packages (v.1.2.1335 with R v.3.6.1) with a cut off criteria of $p<0.005$. The Kallisto-Sleuth and Kallisto-DESeq2 workflows are based upon a previous publication [51]. For quantification, we used either RPKM (Reads Per Kilobase Million) or TPM (Transcripts Per Kilobase Million) as a measure of transcript abundance. RPKM is reads per million divided by the length of genes in kilobases. For TPM, normalization is done for gene length first, and then for sequencing depth. The RNA-seq data were deposited at the GEO < https://www.ncbi.nlm.nih.gov/geo/> and the accession numbers are GSE118313, GSE132689 and GSE152438.

Seahorse assay

Mitochondrial activity of cINs, glutamatergic neurons or iPSCs was measured using the Seahorse XFp8 analyzer (Agilent Technologies, Santa Clara, CA) according to the manufacturer's instructions. Briefly, 50,000 cells were plated in the XF cell culture miniplate and incubated at 37°C with 5% CO_2. One day before the test, the cartridge with XF calibrant was incubated in a non-CO_2 incubator overnight to equilibrate. Before the assay, the media was changed to the XF assay medium supplemented with 5 mM sodium pyruvate (Thermo Scientific, Waltham, MA), 10 mM glucose (Thermo Scientific, Waltham, MA), and 2 mM glutamine, and equilibrated in a non-CO_2 incubator for 1 hour. Oxygen consumption rate (OCR) was monitored through sequential injections of 1 μM oligomycin, 0.3 μM FCCP and 1 μM rotenone/antimycin A (Seahorse XF Cell Mito Stress Test Kit, Agilent, Santa Clara, CA). The various parameters of mitochondrial activity were calculated as illustrated in Extended Data 5A–B (Basal Respiration=baseline OCR-Rotenone/antimycin A OCR, ATP production=Baseline OCR-Oligomycin OCR, Maximum Respiration=FCCP OCR-Rotenone/antimycin A OCR and glycolytic reserve= Oligomycin ECAR – Baseline ECAR). The result was normalized to total protein levels quantified using a BCA protein assay (Thermo Scientific, Cambridge, MA). For analysis of oxidative phosphorylation in

cINs cultured in activated microglia-conditioned media using a Seahorse analyzer, cINs were incubated with or without conditioned media for 1h before assay.

For analysis of oxidative phosphorylation in cINs with overexpression of *CTGF* and *THBS1*, cINs were seeded on PLO/FN-coated Seahorse plates (50,000 cells per well) in B27GB media. The next day, cINs were transfected with pMax-GFP (Lonza) as a control vector or *CTGF*-expressing vector (Cat# HG13612-NF, Sino Biological) and *THBS1*-expresing vector (Cat# HG10508-NF, Sino Biological) using 1mg/ml PEI (Polysciences, Inc.). For transfection, 0.3ug total plasmid DNAs were diluted in 50ul of 150 mM NaCl and 0.3ug PEI was diluted in 50ul of 150mM NaCl solution, followed by gentle addition of the diluted PEI to the diluted DNAs. Following 10 minutes' incubation at RT, the mixture was added to cINs in B27GB media. One hour after transfection, the media was changed with fresh B27GB media and the next day transfected cINs were analyzed for mitochondrial function using Seahorse analyzer. For testing siRNA-mediated knock down of *CTGF* and *THBS1* cultured in activated microglia-conditioned media, cINs were transfected with 25nM negative-control siRNA (Cat# 4611G, Ambion) or 12.5nM *CTGF* siRNA (Cat# 4390824, ThermoFisher) and 12.5nM *THBS1* siRNA (Cat# 4392420, ThermoFisher) using 1mg/ml PEI (Polysciences, Inc.) as described above and analyzed for mitochondrial function the next day. CTGF and THBS1 are both secreted proteins, and thus all the cells in the culture are affected by the release of over-expressed proteins or decrease in released proteins by siRNA Knockdown, regardless of whether each cell is directly transfected or not.

Immunocytochemistry/Arborization analysis/Synapse analysis

cINs, glutamatergic neurons or iPSCs on coverslips were fixed using 4% paraformaldehyde (PFA, Electron Microscopy Sciences, Hatfield, PA) for 10 min, washed with PBS and used for staining. The spheres at different differentiation stages were fixed by 4% PFA for 15 min, rinsed with PBS, cryo-protected in the 30% sucrose (Thermo Fisher, Waltham, MA, USA) overnight at 4°C, mounted on the chuck using the O.C.T. Compound (Thermo Fisher, Waltham, MA, USA) and cryosectioned at 40 μm using a Leica CM1850 cryostat (Leica Biosystem, Buffalo Grove, IL, USA). Fixed cells or sphere sections were incubated with blocking/permeabilization buffer (PBS with 10% normal serum and 0.1% Triton X-100) for 10 min. The samples were then incubated in primary antibodies in antibody dilution buffer (PBS containing 2% normal serum) overnight at 4°C. The detailed information of the antibodies used are as follows; GAD1 (AB1511, 1:1,000, Millipore, validated in [18]), SOX6 (AB5805, 1:1,000, Millipore, validated in [18]), VGAT (131003, 1:1,000, Synaptic Systems, validated in [18]), Gephyrin (147011, 1:1,000, validated in [18]), VGLUT1 (73-066, 1:1,000, UC Davis/NIH NeuroMab, validated in [18]), GABA (20094, 1:1,000, IMMUNOSTAR, https://www.immunostar.com/shop/content/pdf/20094-1418001.pdf), Glutamate (G6642, 1:1,000, Sigma-Aldrich, validated in [18]), β-Tubulin III (802001, 1:1,000, Covance, validated in [18]), Iba1 (019-19741, 1:1,000, FUJIFILM Wako, https://fujifilmcdi.com/products-services/icell-products/anti-iba/), OLIG2 (AB9610, 1:1,000, Millipore, validated in [18]), GFAP (N206A/8, 1:1,000, UC Davis/NIH NeuroMab, https://www.antibodiesinc.com/products/gfap-n206a-8), CHAT (AB114P, 1:1,000, Chemicon, validated in [18]), TH (P40101-150, 1:1,000, Pel-Freez, validated in [18]), 5-HT (20080, 1:1,000, IMMUNOSTAR, validated in [18]) and VIP (20077, 1:1,000, IMMUNOSTAR, validated in [18]) as listed in Supplementary Table 12. More

information on antibody diultion and validation is in the Life Sciences Reporting Summary. After washing with PBS, cells were incubated with fluorescently labeled secondary antibodies and DAPI (Invitrogen, Waltham, MA, USA) in antibody dilution buffer for 1h at room temperature. Following the PBS wash, the samples were mounted with Fluoromount-G (SouthernBiotech, Birmingham, AL, USA). Fluorescent images were taken by the EVOS FL Auto microscope (Life Technologies, Carlsbad, CA) and Leica SPE Confocal Laser Scanning Microscopes (Leica microsystems, Wetzlar, Germany).

For cell counting analysis, Image J software (Version 1.51p, NIH, Bethesda, MD) was used to count the cell number using the multi point function. The experimenters were blind to the sample ID during data collection. Percentages of cells positive for each marker were quantified in relation to DAPI-stained nuclei from three independent differentiations, with a total of at least 500 cells counted for each line.

For arborization analysis, cINs were plated onto the PLO/FN-coated coverslips after 7 weeks' differentiation, followed by infection with a limiting titer (MOI=0.001) of LV-UbiC-GFP virus [52] to label cells only scarcely. After one week's incubation with or without activated microglia-conditioned media, the images of GFP^+ cells were collected by the EVOS microscope. The arborization of each GFP^+ cell was analyzed using Image J software with the Neuron J plugin to get parameters of total neurite length and total branch number.

For synapse analysis, cINs were maintained as organoids and treated with or without activated microglia-conditioned media for one month starting at 2 months after differentiation, and fixed and processed as described above. Images were captured using Leica SPE Confocal Laser Scanning Microscopes with 100x objective and analyzed using IMARIS software (Bitplane, Switzerland), which allows objective counting of synaptic puncta based upon absolute fluorescent intensity. Synaptic puncta positive for VGAT (inhibitory presynaptic) and Gephyrin (inhibitory postsynaptic) were identified with spot diameters of 0.5 μm. A juxtaposition of $GAD1^+VGAT^+$ puncta and $Gephyrin^+$ puncta was determined as inhibitory synapses. The result was expressed as synapse numbers per $GAD1^+$ neuronal surface area (μm^2). We analyzed a total area of 200,057μm^2 for control conditions and a total area of 206,237μm^2 for those cultured in activated microglia-conditioned media. Total counted colocalized puncta numbers were 6770 for control conditions and 5808 for those cultured in activated microglia-conditioned media.

Synaptic GABA release assay

For the synaptic GABA release assay, cINs were seeded on PLO/FN-coated 96well plates (50,000 cells per well) in B27GB media. Cells that had been treated with or without activated HMC3-conditioned media were incubated with media with 50 mM KCL for 30 min, followed by collection of media for GABA release analysis. Parallel cIN cultures were treated in addition with 200nM tetrodotoxin (TTX, Hello Bio), followed by media collection for determining non-synaptic GABA release in the absence of action potential firing. To determine the levels of total GABA amount in cultured media, human GABA ELISA kit (BioVision) was used according to the manufacturer's instruction. Data were normalized by total proteins and action potential firing-dependent GABA release was determined by

subtracting total GABA release with action potential firing-independent GABA release in the presence of TTX.

Statistics

All statistical analyses were performed using GraphPad Prism7 (GraphPad Software, La Jolla, CA), and SAS statistical software (9.4, SAS Institute, Cary, NC). For each figure, the statistical test was justified as appropriate, meeting the assumption of the tests as summarized in Supplementary Table 13. The normal distribution of data was tested using the Shapiro–Wilks test as summarized in Supplementary Table 13. A mixed effect model was used to handle clustering and covariance among correlated samples [53,54] as summarized in Supplementary Table 13. For data sets without correlated samples within a group, a two-tailed paired t-test was used to compare the difference between two means based on a paired samples as shown in Supplementary Table 13. For comparison of HC vs SCZ samples, unpaired t-test was performed as shown in Supplementary Table 13. Some of the data were log-transformed to deal with skewedness as indicated in Supplementary Table 13. For the comparison of group means for more than 2 groups, one-way ANOVA was done and if there was significant difference, posthoc analysis was performed. P-values <0.05 were considered to be statistically significant. More information on statistical analysis can be found in the Life Sciences Reporting Summary.

Study design

No statistical method was used to pre-determine the sample sizes. However, the sample sizes we used in this study are similar to the largest one among previous publications [55]. This sample size was adequate to observe cIN intrinsic transcriptome abnormalities in metabolic gene expression by activated microglia co-culture. Experimental cohorts were chosen based on our selection criteria (Caucasian male SCZ patients treated with Clozapine vs. age- and gender-matched Caucasian male HC) without randomization to reduce variation caused by age, ethnicity and gender (Extended Data 1A and 4A). No data was excluded and the major result of the paper is replicated in the replication cohort (Fig. 1H, Fig. 5H, Extended Data 3 and Extended Data 4). When possible, data analysis was performed by an investigator blind to the testing condition, including for cell counting, arborization analysis and synapse analysis.

Life Science Reporting Summary

Further information on research design is available in the Life Science Reporting Summary linked to this article.

Data availability

The RNA-seq data were deposited at the GEO < https://www.ncbi.nlm.nih.gov/geo/> and the accession numbers are GSE118313, GSE132689 and GSE152438. For human cDNA ensemble database, we used human cDNA fasta file GRCh38 release 87 available at http://www.ensembl.org/info/data/ftp/index.html. The data that support the findings of this study are available from the corresponding authors upon request.

Extended Data

A

Group	ID	Gender	Age	Race	Treatment
HC	272	Male	42	Caucasian	NA
	190	Male	42	Caucasian	NA
	367	Male	21	Caucasian	NA
	226	Male	45	Caucasian	NA
SCZ	67	Male	50	Caucasian	Clozapine
	128	Male	44	Caucasian	Clozapine
	212	Male	42	Caucasian	Clozapine
	162	Male	21	Caucasian	Clozapine

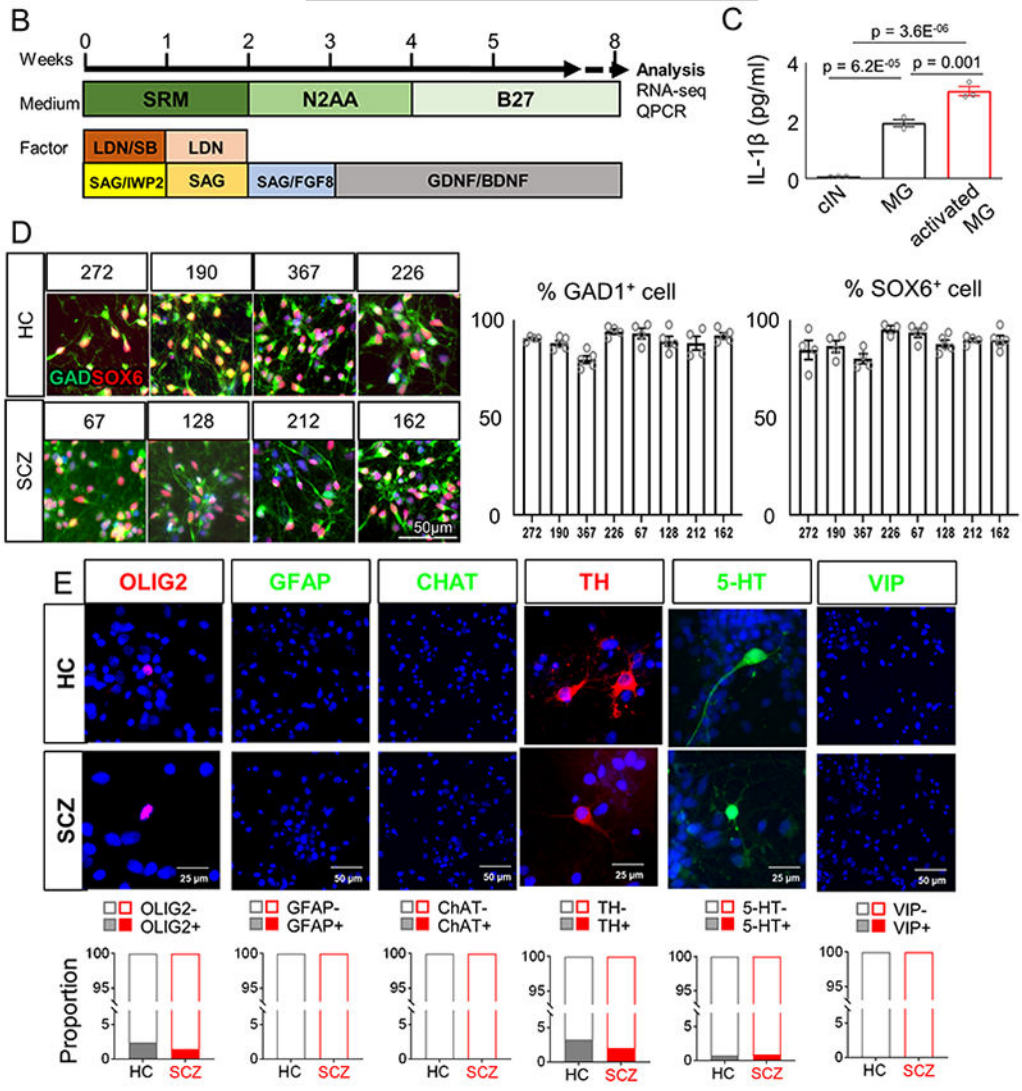

Extended Data Fig. 1. Generation of cINs from human iPSCs.

A. Table of subjects analyzed in pilot study in Fig. 1. HC refers to healthy control subjects and SCZ refers to people with SCZ.

B. Differentiation scheme of cINs from human iPSCs. SRM: serum replacement media, LDN: 100 nM LDN193189, SB: 10 μM SB431542, SAG: 0.1 μM Smoothened agonist, and IWP2: 5 μM Inhibitor of Wnt production-2.

C. ELISA analysis of mouse IL1β release from activated microglia BV2. Data are presented as mean±SEM. One-way ANOVA followed by posthoc analysis using Tukey's multiple comparisons test was used for analysis ($p=0.00000489$ and $n=3$ batches, $f=173.8$, $df=2$).
D. Immunocytochemistry and cell counting analysis of differentiated cINs, demonstrating MGE-derived cIN phenotype with GAD1 and SOX6 expression. Scale bar=50 μm. Percentages of cells positive for each marker were quantified in relation to DAPI-stained total nuclei. For GAD1, Sample sizes (n) as the number of independent differentiations for each line are as follows; 272:4, 190:5, 367:5, 226:4, 67:4, 128:5, 212:4, and 162:5. For SOX6, sample sizes (n) as the number of independent differentiations for each line are as follows; 272:4, 190:4, 367:4, 226:3, 67:4, 128:5, 212:4, and 162:5. At least 500 cells were counted for each line. Data are presented as mean ±SEM.
E. Immunocytochemistry and cell counting analysis of $OLIG2^+$, $GFAP^+$, $CHAT^+$, TH^+, $5\text{-}HT^+$ and VIP^+ cells. Scale bar= 25 or 50 μm. Proportions of $OLIG2^+$ neurons ($p=0.782$, two-sided chi-square test), $GFAP^+$ neurons (Non-detectable for both HC and SCZ), $CHAT^+$ neurons (Non-detectable for both HC and SCZ), TH^+ neurons ($p=0.700$, two-sided chi-square test), $5\text{-}HT^+$ neurons ($p=0.911$, two-sided chi-square test) and VIP+ neurons (non-detectable for both HC and SCZ) between groups. Analysis was repeated at least three times with comparable results.

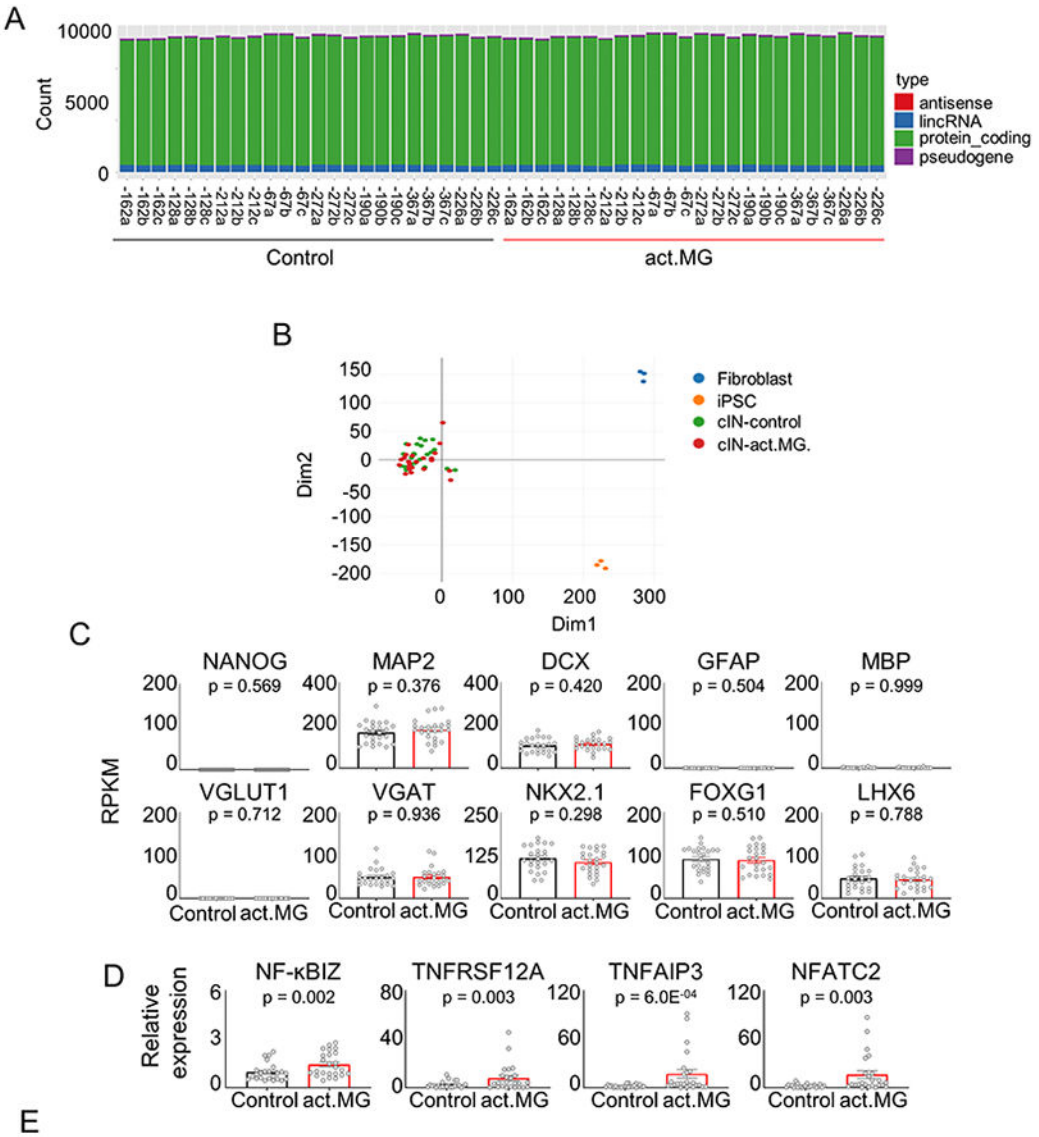

E

ensembl_gene_id	gene_name	SCZ.log2FC	SCZ.Std.Error	SCZ.t.value	SCZ.p.value	SCZ.fdr
ENSG00000144802	NFKBIZ	0.105638298	0.035742818	2.955511185	0.003165205	0.02252794
ENSG00000006327	TNFRSF12A	0.320960695	0.070636847	4.543813999	5.92E-06	0.00017681

F

ensembl_gene_id	gene_name	SCZ.log2FC	SCZ.Std.Error	SCZ.DF	SCZ.t.value	SCZ.p.value	SCZ.fdr
ENSG00000137801	THBS1	0.195501857	0.05344353	1672	3.658101476	0.000261967	0.003384162

Extended Data Fig. 2. RNA-seq analysis of cINs co-cultured with activated microglia.

A. Total identified gene numbers in RNA-seq in Fig. 1.

B. PCA analysis of RNA-seq analysis in Fig. 1 (from 4 HC lines and 4 SCZ lines with 3 independent differentiations from each line as shown in Extended Data 2A).

C. Various phenotype marker expression in cINs with or without co-culture with activated microglia, analyzed by RNA-seq. Gene expression is shown as RPKM, obtained from STAR-featureCount. Differentially expressed genes were analyzed by Kallisto-Sleuth (Wald

test for two-sided significance testing, n=24 batches from 4 HC lines and 4 SCZ lines, each line with 3 independent differentiations). Error bars are SEM.

D. qPCR analysis of inflammatory response gene expression in cINs with or without activated microglia co-culture. Data were normalized by *GAPDH* expression and are presented as mean±SEM. Two-Level Hierarchical Linear Mixed Effect Model after log-transformation was used for analysis (n=24 batches from 4 HC lines and 4 SCZ lines, each line with 3 independent differentiations).

E. Differential expression of inflammatory response genes in HC vs SCZ postmortem PFC from Wang et al [17]

F. Differential expression of THBS1 in HC vs SCZ postmortem PFC from Wang et al[17].

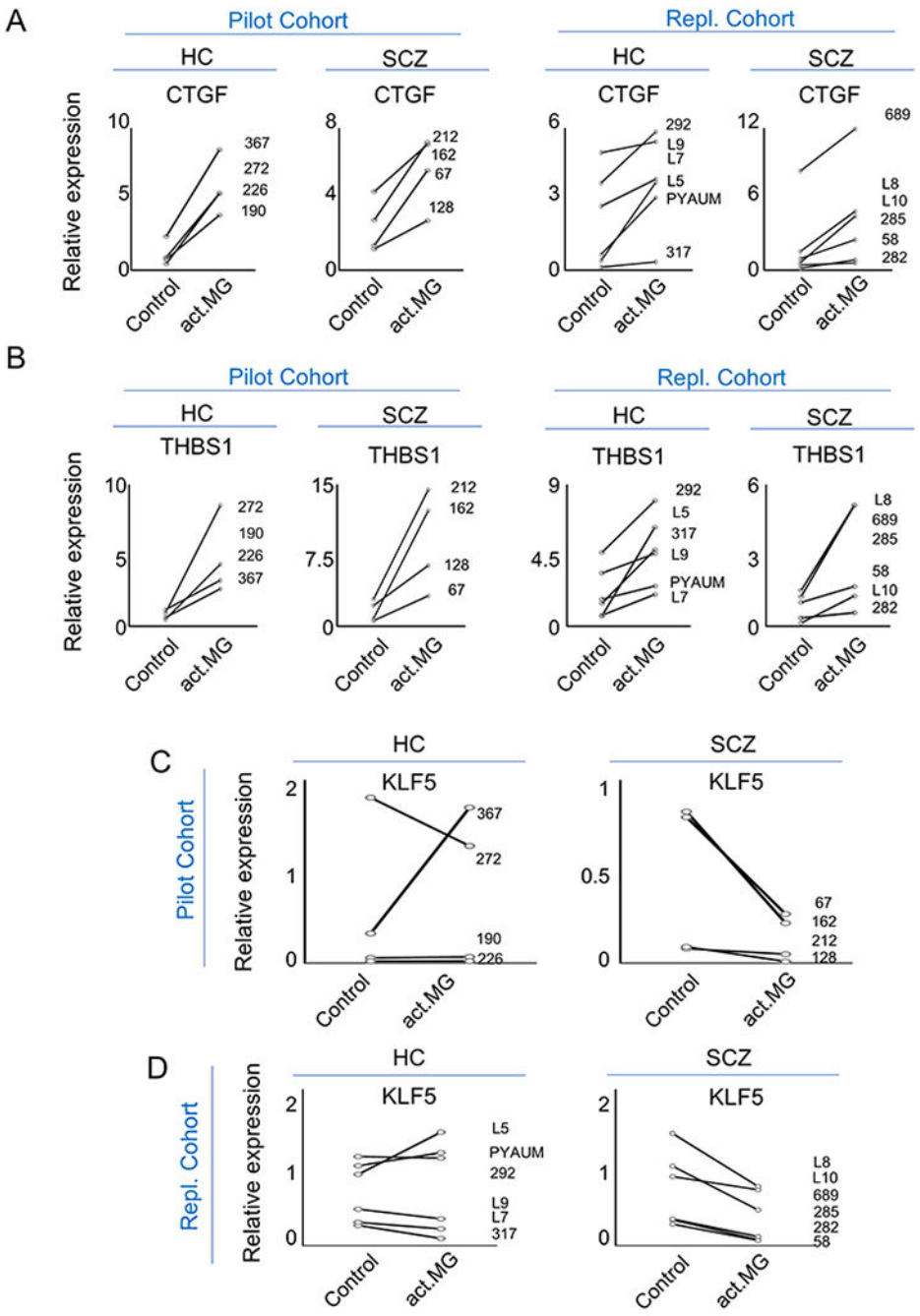

Extended Data Fig. 3. Co-culture with activated microglia results in dysregulated metabolic gene pathways in developmental cINs.

A. Expression of *CTGF* in HC cINs and SCZ cINs with or without co-culture with activated microglia, analyzed by qPCR analysis. Paired data from the same line are connected by a solid line.

B. Expression of *THBS1* in HC cINs and SCZ cINs with or without co-culture with activated microglia, analyzed by qPCR analysis. Paired data from the same line are connected by a solid line.

C. Expression of *KLF5* in HC cINs and SCZ cINs with or without co-culture with activated microglia in the pilot cohort, analyzed by qPCR analysis. Paired data from the same line are connected by a solid line.

D. Expression of *KLF5* in HC cINs and SCZ cINs with or without co-culture with activated microglia in the replication cohort, analyzed by qPCR analysis. Paired data from the same line are connected by a solid line.

A

Group	ID	Gender	Age	Race	Treatment
HC	PYAUM	Male	26	Caucasian	N/A
	317	Male	51	Caucasian	N/A
	L9	Male	38	Caucasian	N/A
	L7	Male	25	Caucasian	N/A
	L5	Male	54	Caucasian	N/A
	292	Male	43	Caucasian	N/A
SCZ	689	Male	32	Caucasian	Clozapine
	285	Male	47	Caucasian	Clozapine
	282	Male	51	Caucasian	Clozapine
	58	Male	43	Caucasian	Clozapine
	L10	Male	37	Caucasian	Clozapine
	L8	Male	50	Caucasian	Clozapine

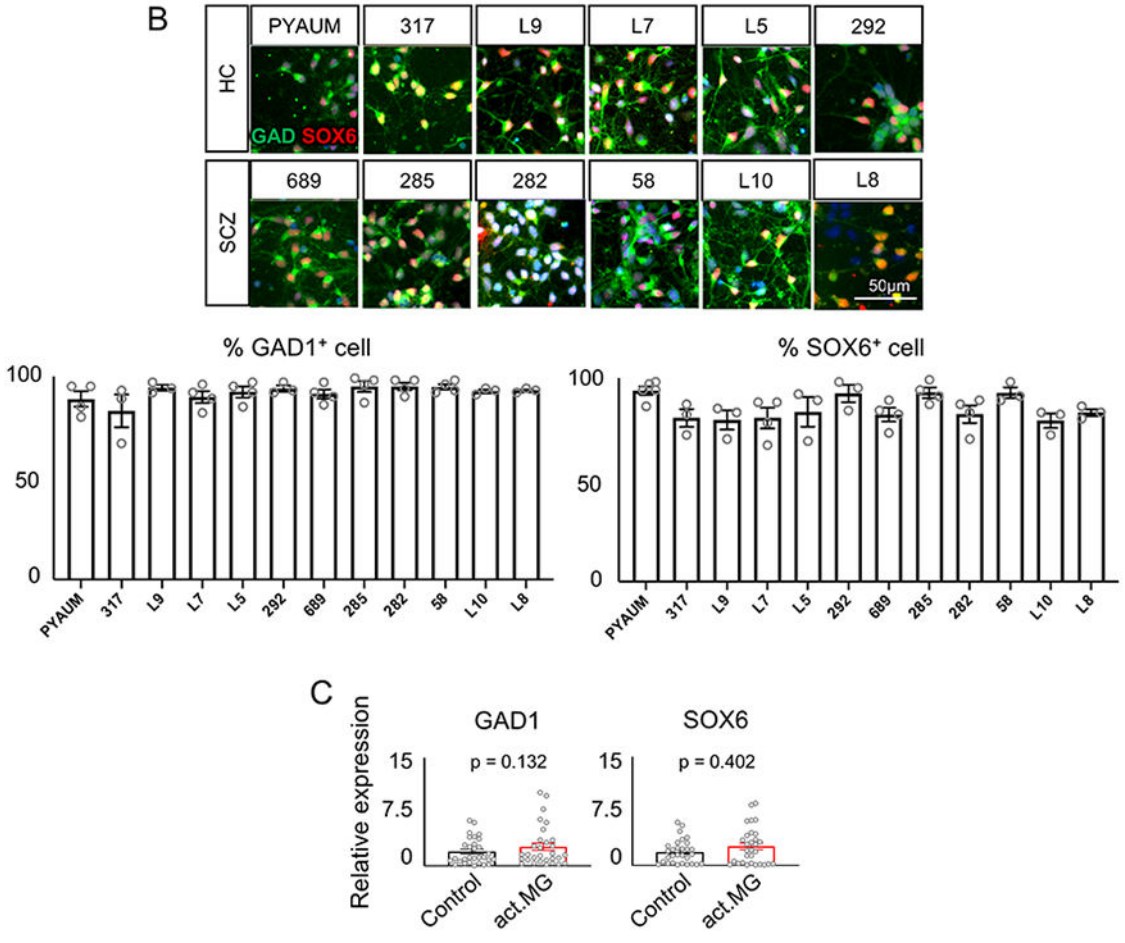

Extended Data Fig. 4. Generation of cINs from human replication cohort iPSCs.

A. Table of subjects analyzed as a replication cohort. HC refers to healthy control subjects and SCZ refers to people with SCZ.

B. Immunocytochemistry and cell counting analysis of generated cINs for expression of GAD1 and SOX6, analyzed after 8 weeks' differentiation. Scale bar= 50 μm. Percentages of cells positive for each marker were quantified in relation to DAPI-stained total nuclei. For GAD1, Sample sizes (n) as the number of independent differentiations for each line are as follows; PYAUM:4, 317:3, L9:3, L7:4, L5:4, 292:3, 689:4, 285:4, 282:4, 58:4, L10:3, and L8:3. For SOX6, sample sizes (n) as the number of independent differentiations for each line are as follows; PYAUM:5 317:3, L9:3, L7:4, L5:3, 292:3, 689:4, 285:4, 282:4, 58:3, L10:3, and L8:3. At least 500 cells were counted for each line. Data are presented as mean ±SEM.

C. qPCR analysis of replication cohort cINs with or without activated microglia co-culture. Data were normalized by *GAPDH* expression and are presented as mean±SEM. Two-Level Hierarchical Linear Mixed Effect Model after log-transformation was used for analysis (n=30 batches from 5 HC lines and 5 SCZ lines, each line with 3 independent differentiations).

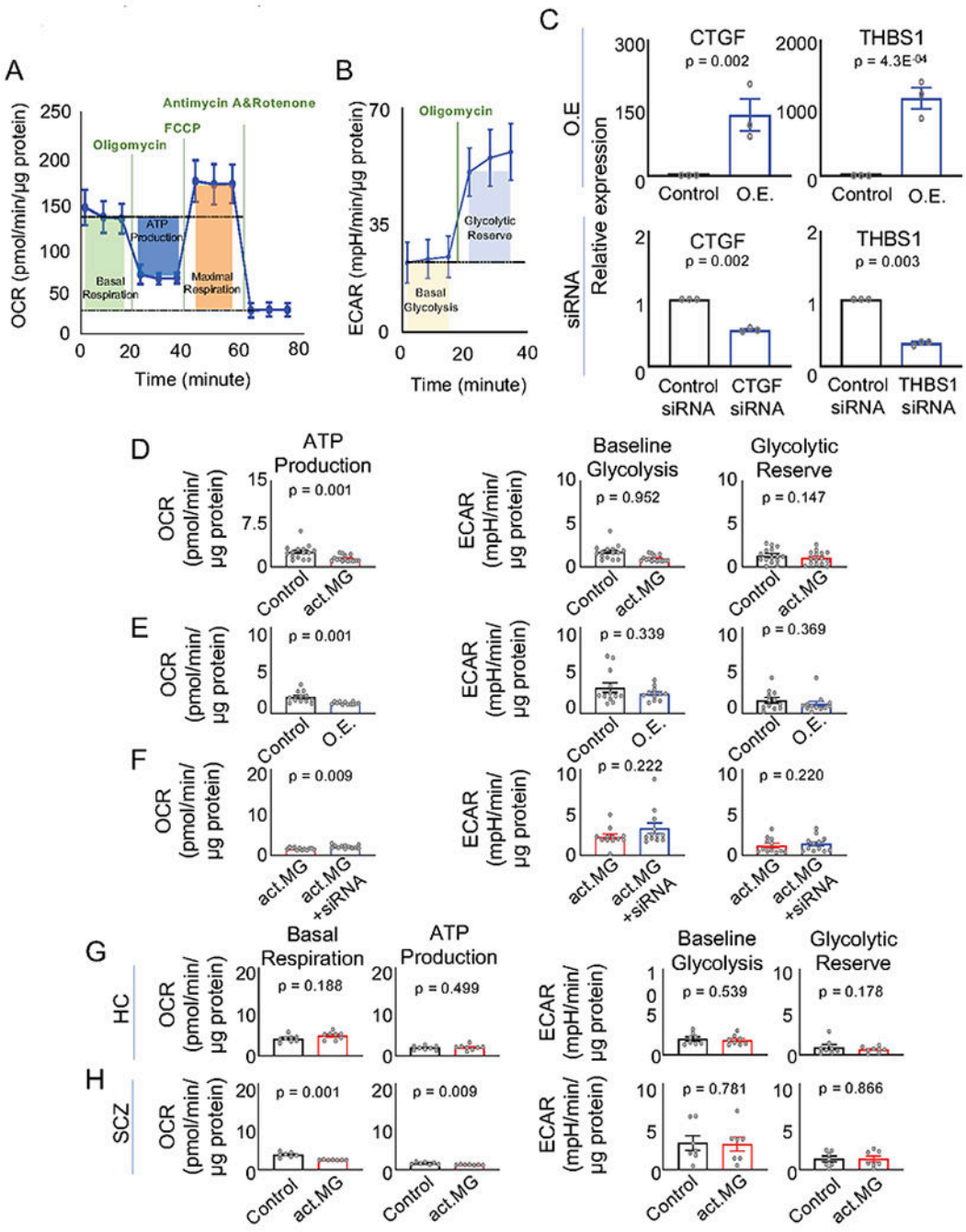

Extended Data Fig. 5. Metabolic analysis of cINs cultured in activated microglia-conditioned media.

A. Schematic diagram of Seahorse analysis OCR data. Basal Respiration=baseline OCR-Rotenone/antimycin A OCR, ATP production=Baseline OCR-Oligomycin OCR and Maximum Respiration=FCCP OCR-Rotenone/antimycin A OCR.

B. Schematic diagram of Seahorse analysis of ECAR data. Glycolytic Reserve= Oligomycin ECAR- Baseline ECAR.

C. Overexpression and siRNA knock down of *CTGF* and *THBS1*, probed by qPCR analysis. Data were normalized by *GAPDH* expression and are presented as mean±SEM. Two-tailed

Ratio paired t-test was used for analysis (n=3 batches, O.E. of *CTGF*: t=19.35, df=2, O.E. of *THBS1*: t=47.92, df=2, siRNA of *CTGF*: t=18.89, df=2, siRNA of *THBS1*: t=17.86, df=2).

D. Analysis of oxidative phosphorylation (ATP Production) and glycolysis (Baseline Glycolysis and Glycolytic Reserve) of cINs cultured with or without activated microglia-conditioned media using a Seahorse Analyzer. Data are presented as mean±SEM. Two-tailed paired t-test after log transformation was used for analysis of ATP Production and Baseline Glycolysis and Two-tailed paired t-test was used for analysis of Glycolytic Reserve (n=15 lines, ATP Production: t=3.978, df=14, Baseline Glycolysis: t=0.06106, df=14, Glycolytic Reserve: t=1.534, df=14).

E. Analysis of oxidative phosphorylation (ATP Production) and glycolysis (Baseline Glycolysis and Glycolytic Reserve) with or without overexpression of CTGF and THBS1 using a Seahorse Analyzer. Data are presented as mean±SEM. Two-tailed paired t-test was used for analysis of ATP Production and Two-tailed paired t-test after log transformation was used for analysis of Baseline Glycolysis and Glycolytic Reserve (n=12 lines, ATP Production: t=4.186, df=11, Baseline Glycolysis: t=0.9984, df=11, Glycolytic Reserve: t=0.9361, df=11).

F. Analysis of oxidative phosphorylation (ATP Production) and glycolysis (Baseline Glycolysis and Glycolytic Reserve) with or without siRNA-mediated knockdown of CTGF and THBS1 using a Seahorse Analyzer. Data are presented as mean±SEM. Two-tailed paired t-test was used for analysis of ATP Production and Two-tailed paired t-test after log transformation was used for analysis of Baseline Glycolysis and Glycolytic Reserve (n=12 lines, ATP Production: t=3.164, df=11, Baseline Glycolysis: t=1.293, df=11, Glycolytic Reserve: t=1.300, df=11).

G. Analysis of oxidative phosphorylation (Basal Respiration and ATP Production) and glycolysis (Baseline Glycolysis and Glycolytic Reserve) in HC cINs using a Seahorse Analyzer one week after removal of activated microglia-conditioned media. Data are presented as mean±SEM. Two-tailed paired t-test was used for analysis of Basal Respiration, ATP Production and Baseline Glycolysis. Two-tailed paired t-test after log transformation was used for analysis of Glycolytic Reserve (n=8 lines; Each data point is averaged from 1-4 independent differentiations, Basal Respiration: t=8.404, df=2, ATP Production: t=0.7116, df=7, Baseline Glycolysis: t=0.6444, df=7, Glycolytic Reserve: t=1.495, df=7).

H. Analysis of oxidative phosphorylation (Basal respiration and ATP production) and glycolysis (Baseline glycolysis and glycolysis reserve) in SCZ cINs using a Seahorse Analyzer one week after removal of activated microglia-conditioned media. Data are presented as mean±SEM. Two-tailed paired t-test was used for analysis (n=7 lines, Each data point is averaged from 1-2 independent differentiations, Basal Respiration: t=5.622, df=6, ATP Production: t=3.750, df=6, Baseline Glycolysis: t=0.2902, df=6, Glycolytic Reserve: t=0.1759, df=6).

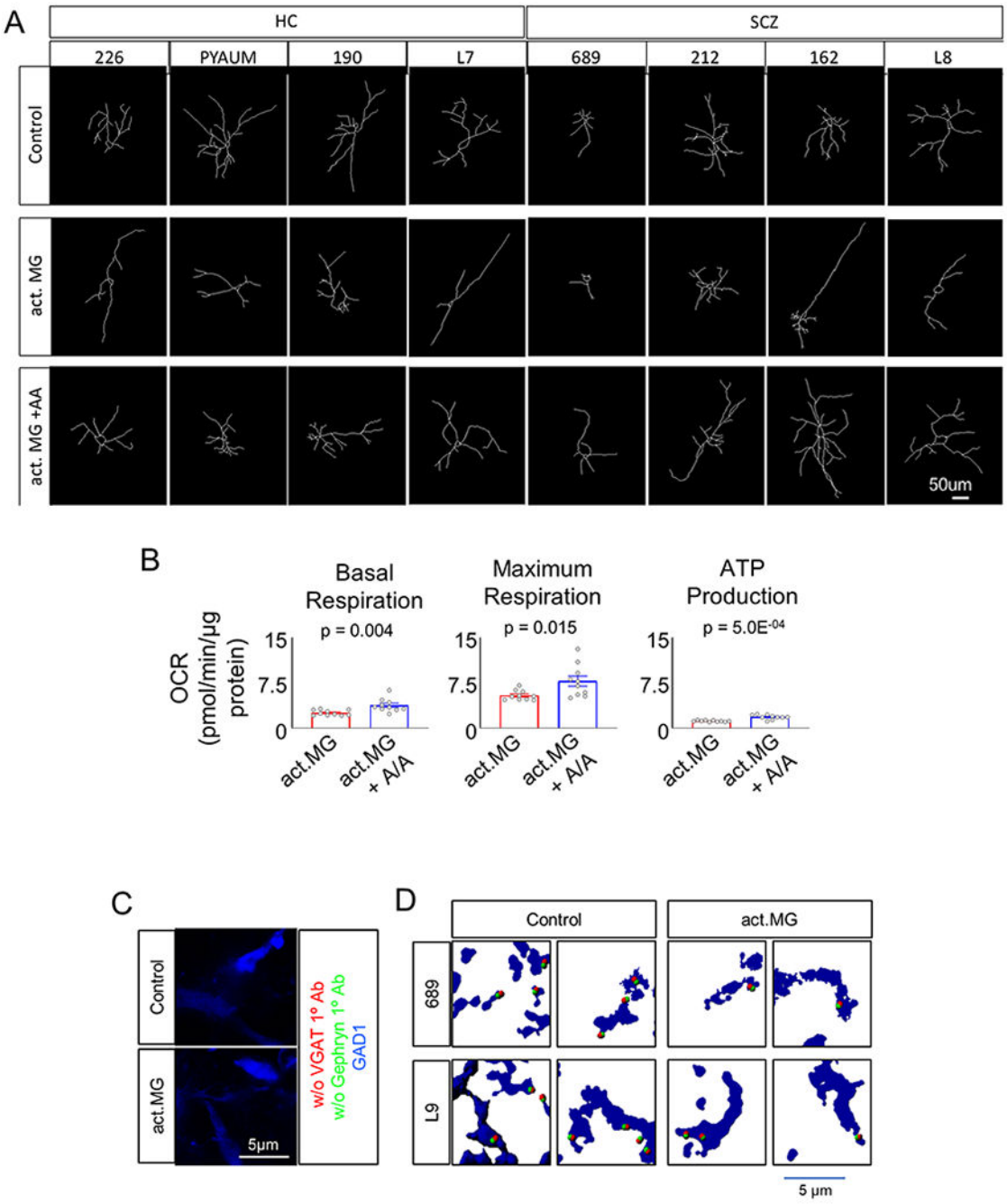

Extended Data Fig. 6. Functional analysis of cINs with activated microglia-conditioned media.

A. Tracing of cINs without activated microglia-conditioned media, with activated microglia-conditioned media or with activated microglia-conditioned media + ALA/ALC treatment. Scale bar= 50 µm. Analysis was repeated at least three times with comparable results.

B. Analysis of mitochondrial function using a Seahorse Analyzer in cINs cultured in activated microglia-conditioned media with or without ALA/ALC treatment. Data are presented as mean±SEM. Two-tailed paired t-test was used for analysis (n=10 lines, Basal

Respiration: t=3.741, df=9, Maximum Respiration: t=2.987, df=9 ATP Production: t=5.281, df=9).

C. Negative control for synapse staining in the absence of primary antibodies for synaptic puncta detection. Scale bar= 5 μm. Analysis was repeated at least three times with comparable results.

D. Synapse analysis of cIN organoids with or without treatment with activated microglia conditioned media. Scale bar= 5 μm. Analysis was repeated at least three times with comparable results.

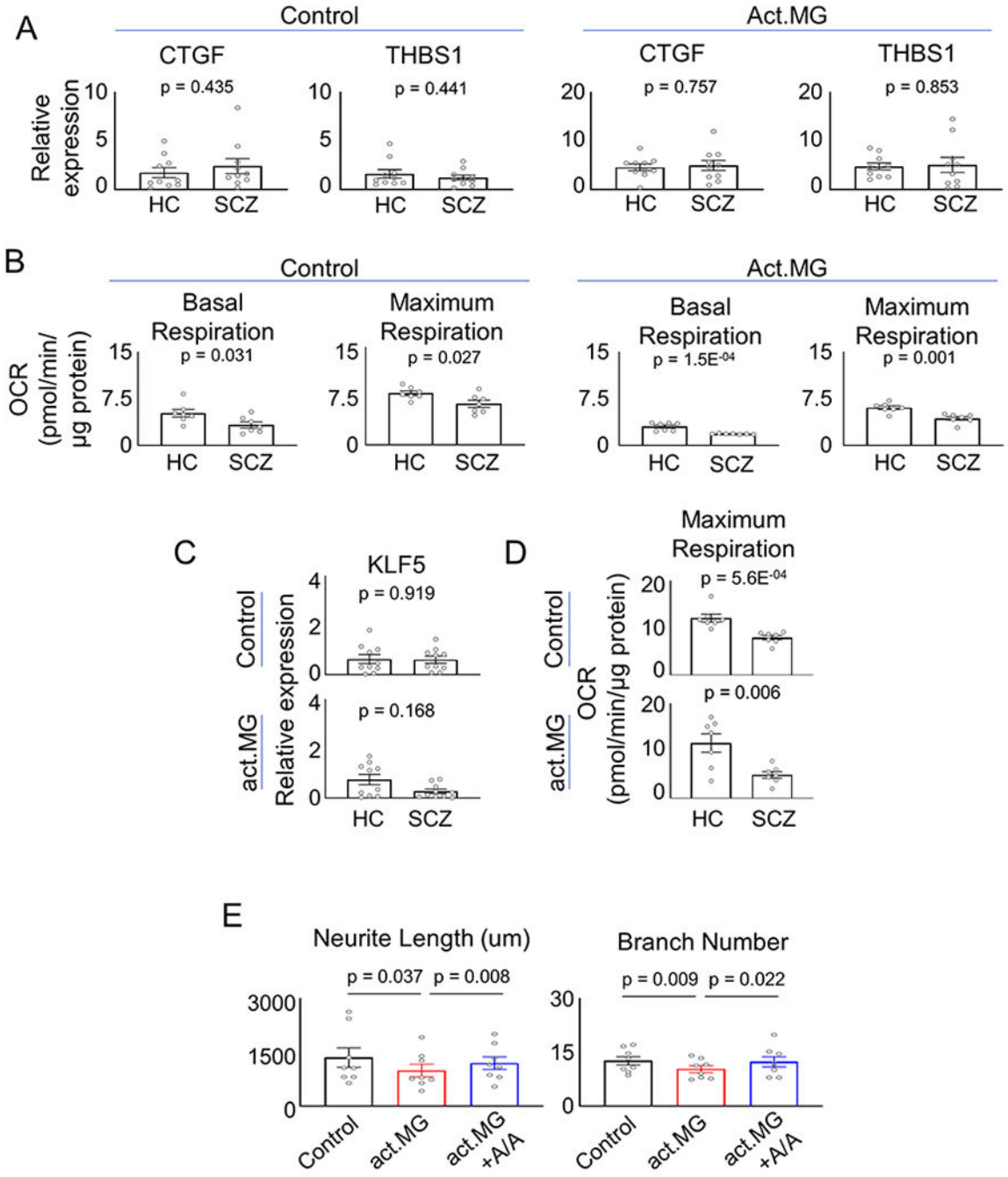

Extended Data Fig. 7. Gene expression analysis and functional analysis of HC and SCZ cINs with or without activated microglia co-culture.

A. qPCR analysis of *CTGF* and *THBS1* expression in HC cINs vs. SCZ cINs with or without activated microglia co-culture. Data were normalized by *GAPDH* expression and are presented as mean±SEM. Two-tailed Unpaired t-test after log transformation was used for analysis of *CTGF* and *THBS1* for control conditions. Two-tailed Unpaired t-test was used for analysis of *CTGF* and *THBS1* for those with activated microglia co-culture (n=10 lines for HC and n=10 lines for SCZ, Each data point is averaged from 3 independent

differentiations, *CTGF* of Control: t=0.7972, df=18, *THBS1* of Control: t=0.7871, df=18, *CTGF* of Act.MG: t=0.3137, df=8, *THBS1* of Act.MG: t=0.1880, df=18).

B. Analysis of oxidative phosphorylation in HC cINs vs. SCZ cINs cultured with or without activated microglia-conditioned media. Data are presented as mean±SEM. Two-tailed Unpaired t-test was used for analysis of Basal Respiration and Maximum Respiration for control conditions. Two-tailed Unpaired t-test after log transformation was used for analysis of Basal Respiration for those cultured in activated microglia-conditioned media. Two-tailed Unpaired t-test was used for analysis of Maximum Respiration for those cultured in activated microglia-conditioned media (n=7 lines for HC and n=7 lines for SCZ, Basal Respiration of Control: t=2.428, df=12, Maximum Respiration of Control: t=2.517, df=12, Basal Respiration of Act.MG: t=5.424, df=12, Maximum Respiration of Act.MG: t=4.262, df=12).

C. qPCR analysis of *KLF5* expression in HC cINs vs. SCZ cINs with or without co-culture with activated microglia one week after the removal of activated microglia co-culture. Data were normalized by *GAPDH* expression and are presented as mean±SEM. Two-tailed Unpaired t-test was used for analysis of *KLF5* qPCR for control conditions and Two-tailed Unpaired t-test after log transformation was used for analysis of *KLF5* qPCR for those with activated microglia co-culture (n=10 lines for HC and n=10 lines for SCZ; Each data point is averaged from 3 independent differentiations, Control: t=0.1021, df=18, Act.MG: t=1.435, df=18).

D. Analysis of oxidative phosphorylation in HC cINs vs. SCZ cINs cultured with or without activated microglia-conditioned media one week after removal of activated microglia-conditioned media. Data are presented as mean±SEM. Two-tailed Unpaired t-test after log transformation was used for analysis of Maximum Respiration for control conditions and Two-tailed Unpaired t-test was used for analysis of Maximum Respiration for those cultured in activated microglia-conditioned media (n=7 lines for HC and n=7 lines for SCZ; Each data point is averaged from 1-4 independent differentiations, Maximum Respiration of Control: t=4.646, df=12, Maximum Respiration of Act.MG: t=3.256, df=12).

E. Arborization analysis of cINs infected with a limiting titer of GFP-expressing lentivirus and cultured without activated microglia-conditioned media, with activated microglia-conditioned media or with activated microglia-conditioned media + ALA/ALC treatment. Data are presented as mean ± SEM. One-way ANOVA, followed by posthoc analysis using Dunnett's multiple comparisons test was used for analysis (n=8 lines consisting of 4 HC lines and 4 SCZ lines, Neurite Length: f=6.116, df=2, Branch Number: f=6.465, df=2).

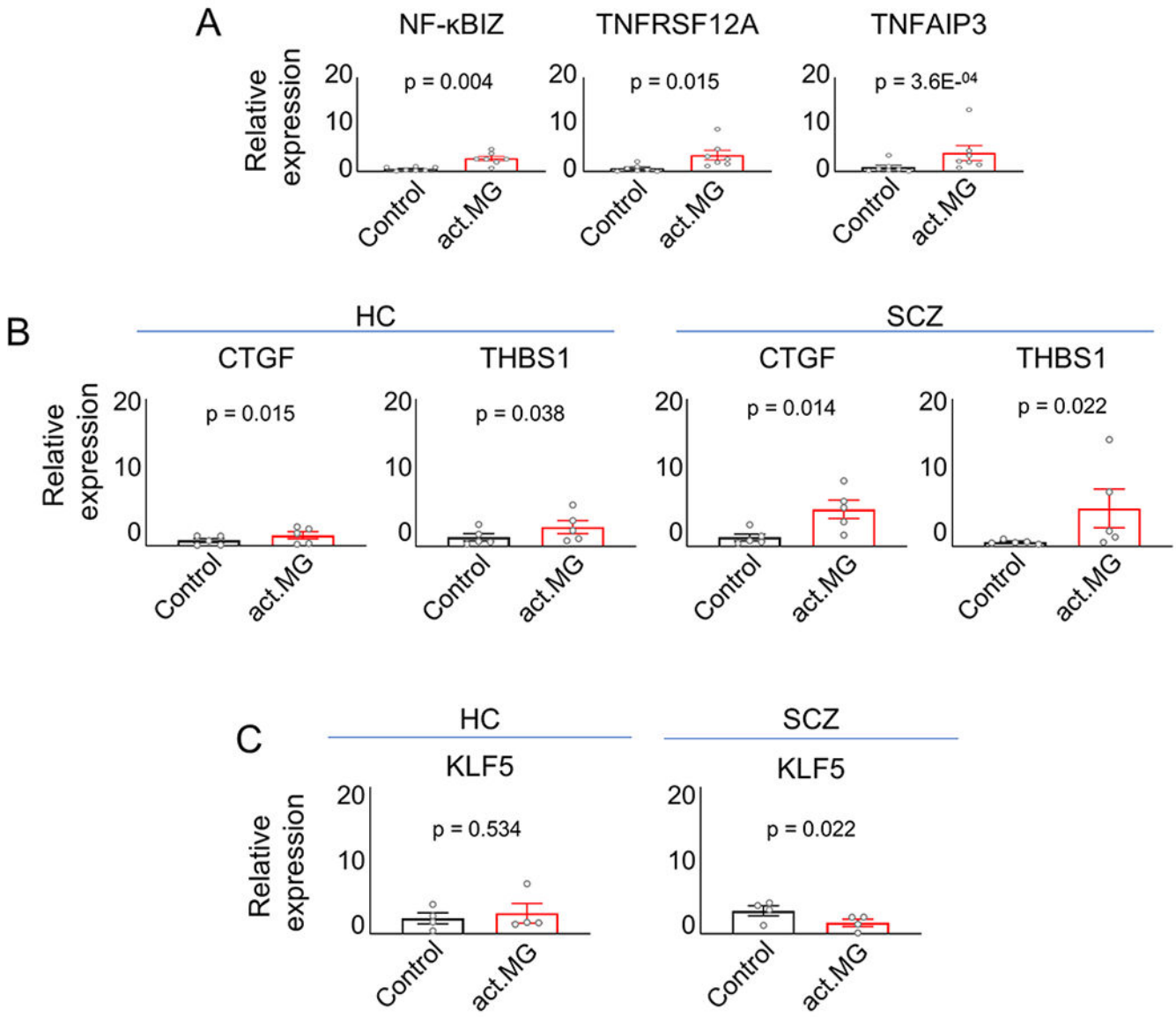

Extended Data Fig. 8. Gene expression analysis of cINs cultured with or without activated HMC3-conditioned media.

A. qPCR analysis of inflammatory gene expression in cINs with and without culturing in activated microglia HMC3-conditioned media. Data were normalized by *GAPDH* expression and are presented as mean±SEM. Two-tailed paired t-test was used for analysis of *NF-κBIZ* and *TNFRSF12A* and Two-tailed paired t-test after log transformation was used for analysis of *TNFAIP3* (n=7 lines, Each data point is averaged from 3 independent differentiations, *NF-κBIZ*: t=4.406, df=6, *TNFRSF12A*: t=3.351, df=6, *TNFAIP3*: t=7.189, df=6).

B. qPCR analysis of *CTGF* and *THBS1* expression in HC cINs or SCZ cINs cultured with or without activated microglia HMC3-conditioned media. Data were normalized by *GAPDH* expression and are presented as mean±SEM. Two-tailed Ratio paired t-test was used for analysis (n=5 lines for HC and n=5 lines for SCZ; Each data point is averaged from 3

independent differentiations, *CTGF* of HC: t=4.018, df=4, *THBS1* of HC: t=3.027, df=4, *CTGF* of SCZ: t=4.131, df=4, *THBS1* of SCZ: t=3.638, df=4).

C. qPCR analysis of *KLF5* expression in HC cINs or SCZ cINs cultured with or without activated microglia HMC3-conditioned media one week after the removal of activated microglia conditioned media. Data were normalized by *GAPDH* expression and are presented as mean±SEM. Two-tailed paired t-test after log transformation was used for analysis of HC *KLF5* qPCR and Two-tailed paired t-test was used for analysis of SCZ *KLF5* qPCR (n=4 lines from HC and n=4 lines from SCZ; Each data point is averaged from 3 independent differentiations, HC: t=0.6992, df=3, SCZ: t=4.364, df=3).

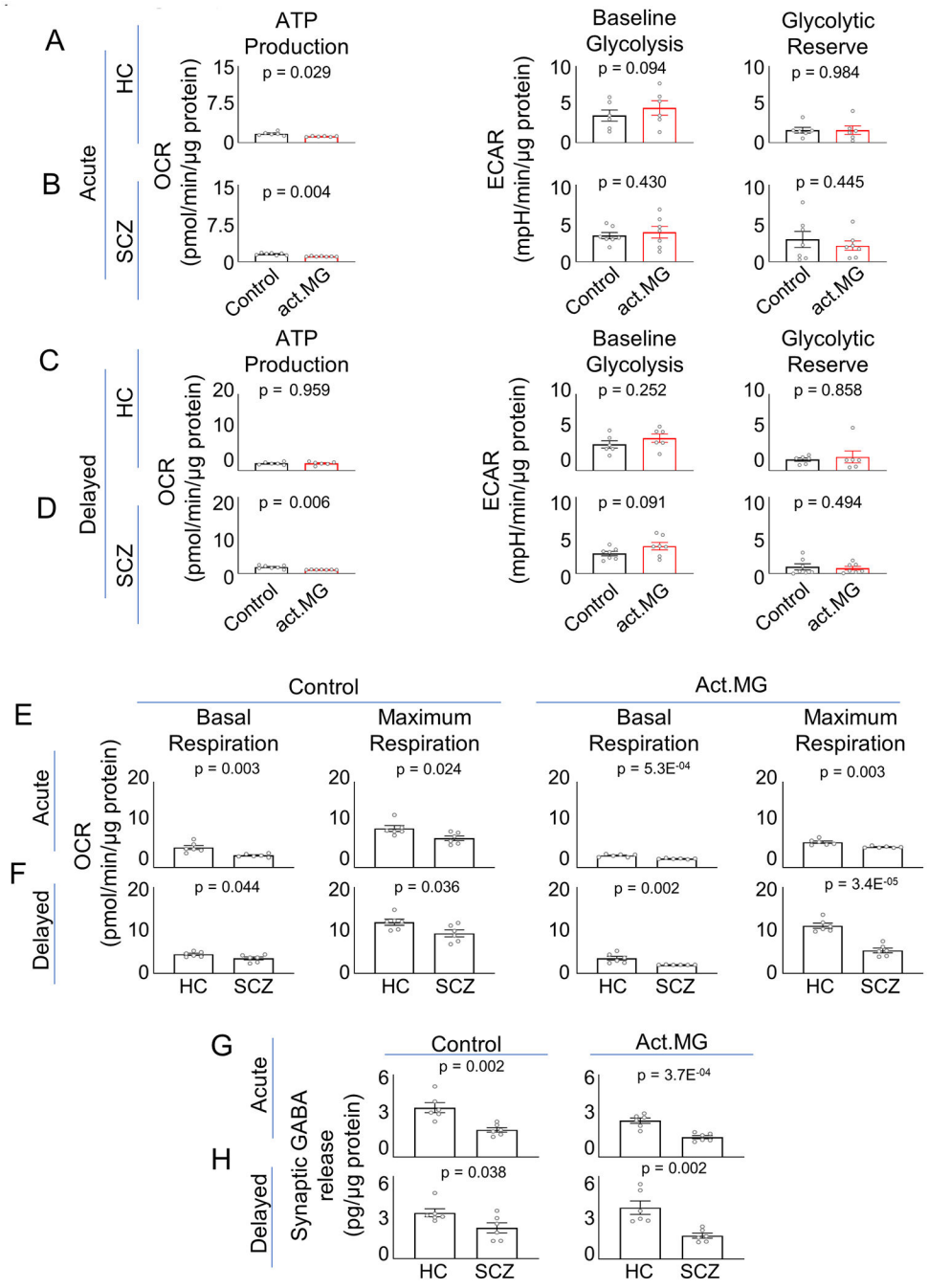

Extended Data Fig. 9. Metabolic analysis of cINs with or without activated HMC3-conditioned media.

A. Analysis of oxidative phosphorylation (ATP Production) and glycolysis (Baseline Glycolysis and Glycolytic Reserve) in HC cINs cultured with or without activated microglia HMC3-conditioned media using a Seahorse Analyzer. Data are presented as mean±SEM. Two-tailed paired t-test was used for analysis (n=6 lines, ATP Production: t=3.028, df=5, Baseline Glycolysis: t=2.064, df=5, Glycolytic Reserve: t=0.02005, df=5).

B. Analysis of oxidative phosphorylation (ATP Production) and glycolysis (Baseline Glycolysis and Glycolytic Reserve) in SCZ cINs cultured with or without activated

microglia HMC3-conditioned media using a Seahorse Analyzer. Data are presented as mean ±SEM. Two-tailed paired t-test was used for analysis (n=7 lines, ATP Production: t=4.421, df=6, Baseline Glycolysis: t=0.8454, df=6, Glycolytic Reserve: t=0.8159, df=6).

C. Analysis of oxidative phosphorylation (ATP Production) and glycolysis (Baseline Glycolysis and Glycolytic Reserve) in HC cINs using a Seahorse Analyzer one week after removal of activated microglia HMC3-conditioned media. Data are presented as mean ±SEM. Two-tailed paired t-test was used for analysis of ATP Production and Baseline Glycolysis and Two-tailed paired t-test after log transformation was used for analysis of Glycolytic Reserve (n=6 lines; Each data point is averaged from 1-4 independent differentiations, ATP Production: t=0.05286, df=5, Baseline Glycolysis: t=1.294, df=5, Glycolytic Reserve: t=0.1876, df=5).

D. Analysis of oxidative phosphorylation (ATP Production) and glycolysis (Baseline Glycolysis and Glycolytic Reserve) in SCZ cINs using a Seahorse Analyzer one week after removal of activated microglia HMC3-conditioned media. Data are presented as mean ±SEM. Two-tailed paired t-test was used for analysis (n=7 lines; Each data point is averaged from 1-2 independent differentiations, ATP Production: t=4.051, df=6, Baseline Glycolysis: t=2.008, df=6, Glycolytic Reserve: t=0.7266, df=6).

E. Analysis of oxidative phosphorylation in HC cINs vs. SCZ cINs cultured with or without activated microglia HMC3-conditioned media. Data are presented as mean±SEM. Two-tailed Unpaired t-test was used for analysis (n=6 lines, Basal Respiration of Control: t=3.743, df=10, Maximum Respiration of Control: t=2.646, df=10, Basal Respiration of Act.MG: t=5.004, df=10, Maximum Respiration of Act.MG: t=3.842, df=10).

F. Analysis of oxidative phosphorylation in HC cINs vs. SCZ cINs culture with or without activated microglia HMC3-conditioned media one week after removal of the activated microglia-conditioned media. Data are presented as mean±SEM. Two-tailed Unpaired t-test was used for analysis of both Basal Respiration and Maximum Respiration for control conditions. Two-tailed Unpaired t-test after log transformation was used for analysis of Basal Respiration for those cultured in activated microglia HMC3-conditioned media. Two-tailed Unpaired t-test was used for analysis of Maximum Respiration for those cultured in activated microglia HMC3-conditioned media (n=6 lines; Each data point is averaged from 1-4 independent differentiations, Basal Respiration of Control: t=2.295, df=10, Maximum Respiration of Control: t=2.409, df=10, Basal Respiration of Act.MG: t=4.066, df=10, Maximum Respiration of Act.MG: t=7.071, df=10).

G. Analysis of action potential firing-dependent synaptic GABA release in HC cINs vs. SCZ cINs cultured with or without activated microglia HMC3-conditioned media. Data are presented as mean±SEM. Two-tailed Unpaired t-test was used for analysis (n=6 lines; Each data point is averaged from 1-3 independent differentiations, Control: t=4.038, df=10, Act.MG: t=5.253, df=10).

H. Analysis of action potential firing-dependent synaptic GABA release in HC cINs vs. SCZ cINs cultured with or without activated microglia HMC3-conditioned media one week after removal of activated microglia-conditioned media. Data are presented as mean±SEM. Two-tailed Unpaired t-test after log transformation was used for control conditions and Two-tailed Unpaired t-test was used for those cultured in activated microglia HMC3-conditioned media (n=6 lines; Each data point is averaged from 1-3 independent differentiations, Control: t=2.379, df=10, Act.MG: t=3923, df=10).

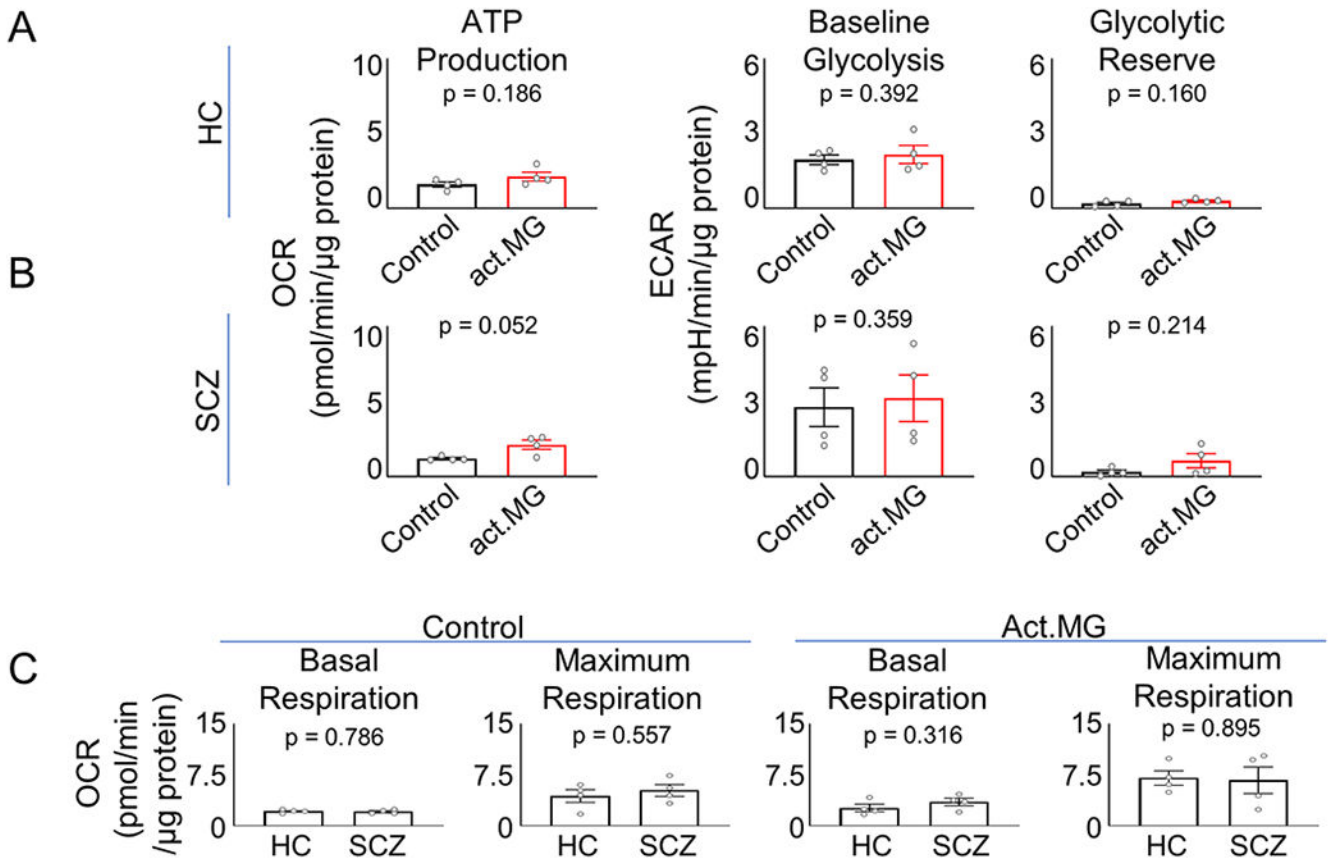

Extended Data Fig. 10. Metabolic analysis of developmental glutamatergic neurons cultured in activated microglia-conditioned media.

A. Analysis of oxidative phosphorylation (ATP Production) and glycolysis (Baseline Glycolysis and Glycolytic Reserve) in HC glutamatergic neurons using a Seahorse Analyzer. Data are presented as mean±SEM. Two-Level Hierarchical Linear Mixed Effect Model was used for analysis (n=4 independent differentiations from 2 lines, each line with 2 independent differentiations).

B. Analysis of oxidative phosphorylation (ATP Production) and glycolysis (Baseline Glycolysis and Glycolytic Reserve) in SCZ glutamatergic neurons using a Seahorse Analyzer. Data are presented as mean±SEM. Two-Level Hierarchical Linear Mixed Effect Model after log transformation was used for analysis of ATP Production and Glycolytic Reserve and Two-Level Hierarchical Linear Mixed Effect Model was used for analysis of Baseline Glycolysis (n=4 independent differentiations from 2 lines, each line with 2 independent differentiations).

C. Analysis of oxidative phosphorylation in HC glutamatergic neurons vs. SCZ glutamatergic neurons cultured with or without activated microglia HMC3-conditioned media. Data are presented as mean±SEM. One-Level Hierarchical Linear Mixed Effect Model was used for analysis (n=4 independent differentiations from 2 lines, each line with 2 independent differentiations).

Supplementary Material

Refer to Web version on PubMed Central for supplementary material.

Acknowledgement

This study was supported by MH107884 (S.C.) and NYSTEM C32607GG (S.C.). We thank Karen F. Berman, MD and Jose Apud, MD PhD at the National Institute of Mental Health for their contribution in providing patient fibroblast samples. We thank Daniel R. Weinberger, M.D. at the Lieber Institute for Brain Development for supplying patient fibroblast samples and for critical review of the manuscript.

References

1. Knuesel I et al. Maternal immune activation and abnormal brain development across CNS disorders. Nature reviews. Neurology 10, 643–660, doi:10.1038/nrneurol.2014.187 (2014). [PubMed: 25311587]
2. Estes ML & McAllister AK Immune mediators in the brain and peripheral tissues in autism spectrum disorder. Nat Rev Neurosci 16, 469–486, doi:10.1038/nrn3978 (2015). [PubMed: 26189694]
3. Hantsoo L, Kornfield S, Anguera MC & Epperson CN Inflammation: A Proposed Intermediary Between Maternal Stress and Offspring Neuropsychiatric Risk. Biol Psychiatry 85, 97–106, doi:10.1016/j.biopsych.2018.08.018 (2019). [PubMed: 30314641]
4. Estes ML & McAllister AK Maternal immune activation: Implications for neuropsychiatric disorders. Science 353, 772–777, doi:papers3://publication/doi/10.1126/science.aag3194 (2016). [PubMed: 27540164]
5. Mallard C, Welin AK, Peebles D, Hagberg H & Kjellmer I White matter injury following systemic endotoxemia or asphyxia in the fetal sheep. Neurochemical research 28, 215–223 (2003). [PubMed: 12608695]
6. Kuypers E et al. Effects of intra-amniotic lipopolysaccharide and maternal betamethasone on brain inflammation in fetal sheep. PLoS ONE 8, e81644, doi:10.1371/journal.pone.0081644 (2013). [PubMed: 24358119]
7. Hutton LC, Castillo-Melendez M, Smythe GA & Walker DW Microglial activation, macrophage infiltration, and evidence of cell death in the fetal brain after uteroplacental administration of lipopolysaccharide in sheep in late gestation. American journal of obstetrics and gynecology 198, 117.e111–111, doi:10.1016/j.ajog.2007.06.035 (2008). [PubMed: 18166323]
8. Benes FM The GABA system in schizophrenia: cells, molecules and microcircuitry. Schizophr Res 167, 1–3, doi:10.1016/j.schres.2015.07.017 (2015). [PubMed: 26255083]
9. Lewis DA, Hashimoto T & Volk DW Cortical inhibitory neurons and schizophrenia. Nat Rev Neurosci 6, 312–324, doi:10.1038/nrn1648 (2005). [PubMed: 15803162]
10. Volk DW & Lewis DA Early developmental disturbances of cortical inhibitory neurons: contribution to cognitive deficits in schizophrenia. Schizophr Bull 40, 952–957, doi:10.1093/schbul/sbu111 (2014). [PubMed: 25053651]
11. Lewis DA et al. Subunit-selective modulation of GABA type A receptor neurotransmission and cognition in schizophrenia. The American journal of psychiatry 165, 1585–1593 (2008). [PubMed: 18923067]
12. Estes ML & McAllister AK Maternal immune activation: Implications for neuropsychiatric disorders. Science 353, 772–777, doi:10.1126/science.aag3194 (2016). [PubMed: 27540164]
13. Hilker R et al. Heritability of Schizophrenia and Schizophrenia Spectrum Based on the Nationwide Danish Twin Register. Biological psychiatry 83, 492–498, doi:10.1016/j.biopsych.2017.08.017 (2018). [PubMed: 28987712]
14. Takahashi K et al. Induction of pluripotent stem cells from adult human fibroblasts by defined factors. Cell 131, 861–872, doi:10.1016/j.cell.2007.11.019 (2007). [PubMed: 18035408]

15. Windrem MS et al. Human iPSC Glial Mouse Chimeras Reveal Glial Contributions to Schizophrenia. Cell Stem Cell 21, 195–208 e196, doi:10.1016/j.stem.2017.06.012 (2017). [PubMed: 28736215]
16. Noh H, Shao ZC, Coyle JT & Chung SM Modeling schizophrenia pathogenesis using patient-derived induced pluripotent stem cells (iPSCs). Bba-Mol Basis Dis 1863, 2382–2387, doi:10.1016/j.bbadis.2017.06.019 (2017).
17. Wang D et al. Comprehensive functional genomic resource and integrative model for the human brain. Science 362, doi:10.1126/science.aat8464 (2018).
18. Shao Z et al. Dysregulated protocadherin-pathway activity as an intrinsic defect in induced pluripotent stem cell-derived cortical interneurons from subjects with schizophrenia. Nat Neurosci 22, 229–242, doi:10.1038/s41593-018-0313-z (2019). [PubMed: 30664768]
19. Ahn S, Kim TG, Kim KS & Chung S Differentiation of human pluripotent stem cells into Medial Ganglionic Eminence vs. Caudal Ganglionic Eminence cells. Methods 101, 103–112, doi:10.1016/j.ymeth.2015.09.009 (2016). [PubMed: 26364591]
20. Ni P et al. iPSC-derived homogeneous populations of developing schizophrenia cortical interneurons have compromised mitochondrial function. Mol Psychiatry, doi:10.1038/s41380-019-0423-3 (2019).
21. Ni P & Chung S Mitochondrial Dysfunction in Schizophrenia. Bioessays 42, e1900202, doi:10.1002/bies.201900202 (2020). [PubMed: 32338416]
22. Choi GB et al. The maternal interleukin-17a pathway in mice promotes autism-like phenotypes in offspring. Science 351, 933–939, doi:10.1126/science.aad0314 (2016). [PubMed: 26822608]
23. Kim S et al. Maternal gut bacteria promote neurodevelopmental abnormalities in mouse offspring. Nature 549, 528–532, doi:10.1038/nature23910 (2017). [PubMed: 28902840]
24. Kim TG et al. Efficient specification of interneurons from human pluripotent stem cells by dorsoventral and rostrocaudal modulation. Stem Cells 32, 1789–1804, doi:10.1002/stem.1704 (2014). [PubMed: 24648391]
25. Gandal MJ et al. Transcriptome-wide isoform-level dysregulation in ASD, schizophrenia, and bipolar disorder. Science 362, doi:10.1126/science.aat8127 (2018).
26. Jun JI & Lau LF Taking aim at the extracellular matrix: CCN proteins as emerging therapeutic targets. Nat Rev Drug Discov 10, 945–963, doi:10.1038/nrd3599 (2011). [PubMed: 22129992]
27. McClain JA, Phillips LL & Fillmore HL Increased MMP-3 and CTGF expression during lipopolysaccharide-induced dopaminergic neurodegeneration. Neurosci Lett 460, 27–31, doi:10.1016/j.neulet.2009.05.044 (2009). [PubMed: 19463894]
28. Meyer U Prenatal poly(i:C) exposure and other developmental immune activation models in rodent systems. Biol Psychiatry 75, 307–315, doi:10.1016/j.biopsych.2013.07.011 (2014). [PubMed: 23938317]
29. Kong P et al. Thrombospondin-1 regulates adiposity and metabolic dysfunction in diet-induced obesity enhancing adipose inflammation and stimulating adipocyte proliferation. American journal of physiology. Endocrinology and metabolism 305, E439–450, doi:10.1152/ajpendo.00006.2013 (2013). [PubMed: 23757408]
30. Gosselin D et al. An environment-dependent transcriptional network specifies human microglia identity. Science 356, eaal3222, doi:10.1126/science.aal3222 (2017). [PubMed: 28546318]
31. Cai Q & Tammineni P Mitochondrial Aspects of Synaptic Dysfunction in Alzheimer's Disease. Journal of Alzheimer's disease : JAD 57, 1087–1103, doi:10.3233/jad-160726 (2017). [PubMed: 27767992]
32. Mendoza E et al. In vivo mitochondrial inhibition alters corticostriatal synaptic function and the modulatory effects of neurotrophins. Neuroscience 280, 156–170, doi:10.1016/j.neuroscience.2014.09.018 (2014). [PubMed: 25241069]
33. Du H et al. Early deficits in synaptic mitochondria in an Alzheimer's disease mouse model. Proc Natl Acad Sci U S A 107, 18670–18675, doi:10.1073/pnas.1006586107 (2010). [PubMed: 20937894]
34. Oishi Y et al. SUMOylation of Kruppel-like transcription factor 5 acts as a molecular switch in transcriptional programs of lipid metabolism involving PPAR-delta. Nat Med 14, 656–666, doi:10.1038/nm1756 (2008). [PubMed: 18500350]

35. Drosatos K et al. Cardiac Myocyte KLF5 Regulates Ppara Expression and Cardiac Function. Circulation research 118, 241–253, doi:10.1161/circresaha.115.306383 (2016). [PubMed: 26574507]

36. Dello Russo C et al. The human microglial HMC3 cell line: where do we stand? A systematic literature review. J Neuroinflammation 15, 259, doi:10.1186/s12974-018-1288-0 (2018). [PubMed: 30200996]

37. Gumusoglu SB & Stevens HE Maternal Inflammation and Neurodevelopmental Programming: A Review of Preclinical Outcomes and Implications for Translational Psychiatry. Biol Psychiatry 85, 107–121, doi:10.1016/j.biopsych.2018.08.008 (2019). [PubMed: 30318336]

38. Tsuyama T, Tsubouchi A, Usui T, Imamura H & Uemura T Mitochondrial dysfunction induces dendritic loss via eIF2alpha phosphorylation. J Cell Biol 216, 815–834, doi:10.1083/jcb.201604065 (2017). [PubMed: 28209644]

39. Montalvo GB, Artalejo AR & Gilabert JA ATP from subplasmalemmal mitochondria controls Ca2+-dependent inactivation of CRAC channels. J Biol Chem 281, 35616–35623, doi:10.1074/jbc.M603518200 (2006). [PubMed: 16982621]

40. Vanden Berghe P, Kenyon JL & Smith TK Mitochondrial Ca2+ uptake regulates the excitability of myenteric neurons. J Neurosci 22, 6962–6971, doi:20026707 (2002). [PubMed: 12177194]

41. Demaurex N, Poburko D & Frieden M Regulation of plasma membrane calcium fluxes by mitochondria. Biochim Biophys Acta 1787, 1383–1394, doi:10.1016/j.bbabio.2008.12.012 (2009). [PubMed: 19161976]

42. Pei L & Wallace DC Mitochondrial Etiology of Neuropsychiatric Disorders. Biol Psychiatry 83, 722–730, doi:10.1016/j.biopsych.2017.11.018 (2018). [PubMed: 29290371]

43. Devaraju P et al. Haploinsufficiency of the 22q11.2 microdeletion gene Mrpl40 disrupts short-term synaptic plasticity and working memory through dysregulation of mitochondrial calcium. Molecular Psychiatry 22, 1313, doi:10.1038/mp.2016.7510.1038/mp.2016.75https://www.nature.com/articles/mp201675#supplementary-informationhttps://www.nature.com/articles/mp201675#supplementary-information (2016). [PubMed: 27184122]

44. Robicsek O et al. Isolated Mitochondria Transfer Improves Neuronal Differentiation of Schizophrenia-Derived Induced Pluripotent Stem Cells and Rescues Deficits in a Rat Model of the Disorder. Schizophr Bull 44, 432–442, doi:10.1093/schbul/sbx077 (2018). [PubMed: 28586483]

45. Inan M et al. Energy deficit in parvalbumin neurons leads to circuit dysfunction, impaired sensory gating and social disability. Neurobiol Dis 93, 35–46, doi:10.1016/j.nbd.2016.04.004 (2016). [PubMed: 27105708]

46. Fernandez A et al. Mitochondrial Dysfunction Leads to Cortical Under-Connectivity and Cognitive Impairment. Neuron, doi:10.1016/j.neuron.2019.04.013 (2019).

47. Lin-Hendel EG, McManus MJ, Wallace DC, Anderson SA & Golden JA Differential Mitochondrial Requirements for Radially and Non-radially Migrating Cortical Neurons: Implications for Mitochondrial Disorders. Cell Rep 15, 229–237, doi:10.1016/j.celrep.2016.03.024 (2016). [PubMed: 27050514]

48. Schizophrenia Working Group of the Psychiatric Genomics, C. Biological insights from 108 schizophrenia-associated genetic loci. Nature 511, 421–427, doi:10.1038/nature13595 (2014). [PubMed: 25056061]

49. Vuillermot S, Luan W, Meyer U & Eyles D Vitamin D treatment during pregnancy prevents autism-related phenotypes in a mouse model of maternal immune activation. Molecular autism 8, 9, doi:10.1186/s13229-017-0125-0 (2017). [PubMed: 28316773]

50. Glass CK, Saijo K, Winner B, Marchetto MC & Gage FH Mechanisms Underlying Inflammation in Neurodegeneration. Cell 140, 918–934, doi:10.1016/j.cell.2010.02.016 (2010). [PubMed: 20303880]

Online Methods References

51. Bray NL, Pimentel H, Melsted P & Pachter L Near-optimal probabilistic RNA-seq quantification. Nat Biotechnol 34, 525–527, doi:10.1038/nbt.3519 (2016). [PubMed: 27043002]

52. Hong S et al. Functional analysis of various promoters in lentiviral vectors at different stages of in vitro differentiation of mouse embryonic stem cells. Mol Ther 15, 1630–1639, doi:10.1038/sj.mt.6300251 (2007). [PubMed: 17609656]

53. Herring AH Applied Longitudinal Analysis, 2nd Edition, by Fitzmaurice Garrett M., Laird Nan M., and Ware James H., John Wiley & Sons, 2011. Journal of Biopharmaceutical Statistics 23, 940–941, doi:10.1080/10543406.2013.789817 (2013).

54. Laird NM & Ware JH Random-effects models for longitudinal data. Biometrics 38, 963–974 (1982). [PubMed: 7168798]

55. Jensen KP et al. Alcohol-responsive genes identified in human iPSC-derived neural cultures. Transl Psychiatry 9, 96, doi:10.1038/s41398-019-0426-5 (2019). [PubMed: 30862775]

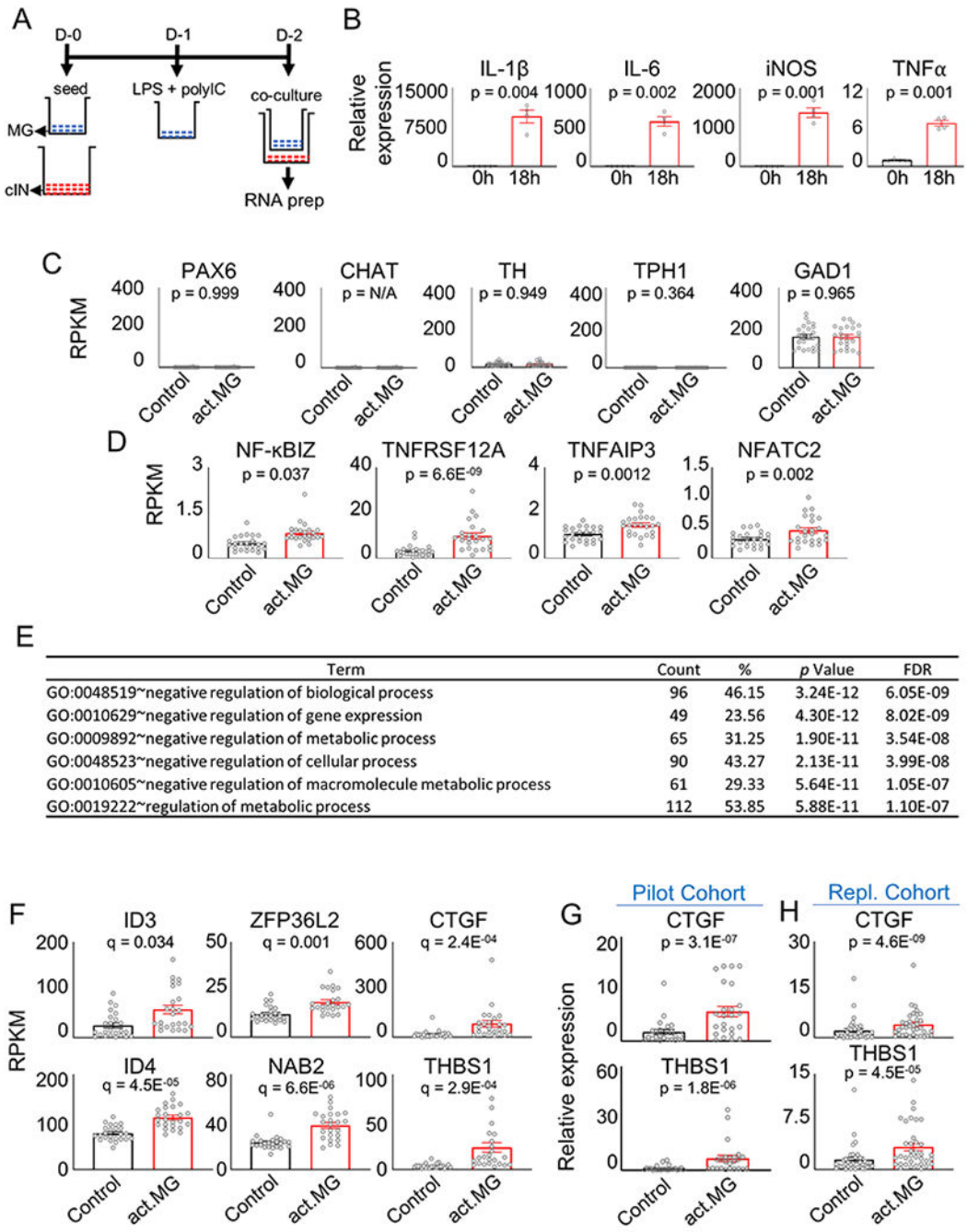

Fig. 1. Co-culture with activated microglia induces metabolic gene dysregulation in developmental cINs.

A. Scheme for coculturing developmental cINs with activated microglia. Microglial cells were activated in the tissue culture insert and co-cultured with cINs via insert without direct contact.

B. qPCR analysis of inflammatory gene expression before and after activating microglial cells. Data were normalized by *GAPDH* expression and are presented as mean±SEM. Two-tailed paired t-test was used for analysis (n=4 batches of independent activation and harvest, *IL-1β*: t=7.770, df=3, *IL-6*: t=9.542, df=3, *iNOS*: t=11.07, df=3, *TNF α*: t=12.05, df=3).

C. Various phenotype marker expression in cINs with or without co-culture with activated microglia, analyzed by RNA-seq. Gene expression is shown as RPKM (Reads Per Kilobase of transcript), obtained from STAR-featureCount. Differentially expressed genes were analyzed by Kallisto-Sleuth (Wald test for two-sided significance testing, n=24 batches from 4 HC lines and 4 SCZ lines, each line with 3 independent differentiations). Error bars are SEM.

D. Inflammatory response gene expression in cINs with or without activated microglia co-culture, analyzed by RNA-seq. Gene expression is shown as RPKM, obtained from STAR-featureCount. Differentially expressed genes were analyzed by Kallisto-Sleuth (Wald test for two-sided significance testing, n=24 batches from 4 HC lines and 4 SCZ lines, each line with 3 independent differentiations). Error bars are SEM.

E. Pathway analysis of enriched genes with differential expression using DAVID (https://david.ncifcrf.gov/summary.jsp). Significant enrichment was tested by the Fisher's Exact Test. FDR: false discovery rate with Benjamini-Hochberg multiple testing.

F. RNA-seq analysis of cINs with or without activated microglia co-culture. Gene expression is shown as RPKM, obtained from STAR-featureCount. Differentially expressed genes were analyzed by Kallisto-Sleuth (Wald test for two-sided significance testing, n=24 batches from 4 HC lines and 4 SCZ lines, each line with 3 independent differentiations). Error bars are SEM.

G. qPCR analysis of *CTGF* and *THBS1* expression in cINs with or without activated microglia co-culture. Data were normalized by *GAPDH* expression and are presented as mean±SEM. Two-Level Hierarchical Linear Mixed Effect Model after log-transformation was used for analysis (n=24 batches from 4 HC lines and 4 SCZ lines, each line with 3 independent differentiations).

H. qPCR analysis of replication cohort cINs with or without activated microglia co-culture. Data were normalized by *GAPDH* expression and are presented as mean±SEM. Two-Level Hierarchical Linear Mixed Effect Model after log-transformation was used for analysis (n=36 batches from 6 HC lines and 6 SCZ lines, each line with 3 independent differentiations).

The lines used in these experiments are summarized in Supplementary Table 10 and Extended Data. 1A.

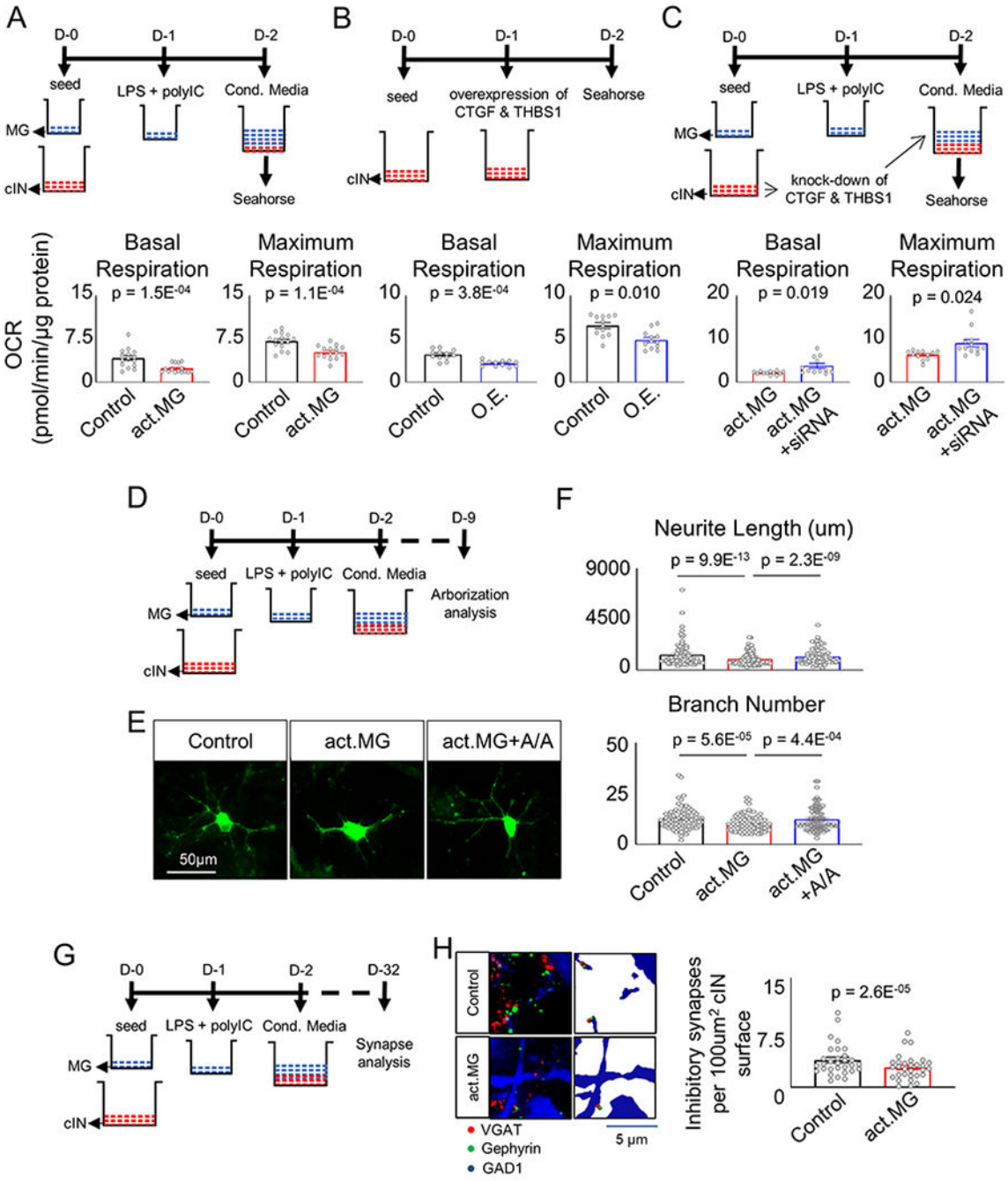

Fig. 2. Co-culture with activated microglia results in compromised metabolism in developmental cINs.

A. Analysis of mitochondrial function using a Seahorse Analyzer, showing significant decreases in mitochondrial function in cINs cultured in activated microglia-conditioned media. Data are presented as mean±SEM. Two-tailed paired t-test after log transformation was used for analysis of Basal Respiration and Two-tailed paired t-test was used for analysis of Maximum Respiration (n=15 lines, Basal Respiration: t=5.129, df=14, Maximum Respiration: t=5.295, df=14).

B. Analysis of mitochondrial function of cINs with overexpression of *CTGF* and *THBS1* using Seahorse Analyzer. Data are presented as mean±SEM. Two-tailed paired t-test was used for analysis (n=12 lines, Basal Respiration: t=5.030, df=11, Maximum Respiration: t=3.076, df=11).

C. Analysis of mitochondrial function of cINs cultured in activated microglia-conditioned media with *CTGF* and *THBS1* knock down using Seahorse Analyzer. Data are presented as mean±SEM. Two-tailed paired t-test after log transformation was used for analysis (n=12 lines, Basal Respiration: t=2.721, df=11, Maximum Respiration: t=2.612, df=11).

D. Scheme of arborization analysis of cINs infected with a limiting titer of GFP-expressing lentivirus cultured with or without activated microglia-conditioned media.

E. Representative images of arborization analysis of cINs cultured without activated microglia-conditioned media, with activated microglia-conditioned media or with activated microglia-conditioned media + ALA/ALC treatment. Scale bar= 50 μm. Analysis was repeated at least three times with comparable results.

F. Arborization analysis of cINs without activated microglia-conditioned media, with activated microglia-conditioned media or with activated microglia-conditioned media + ALA/ALC treatment. Images were analyzed using ImageJ with the Neuron J plugin. Center and error bars show mean ± SEM. Data were collected from 4 HC lines and 4 SCZ lines, each line with 10 neurons (n=80 neurons). Two-Level Hierarchical Linear Mixed Effect Model after log-transformation was used for analysis of neurite length and Two-Level Hierarchical Mixed Effect Log-Linear Model was used for analysis of branch number, followed by Dunnett's test as a post hoc analysis. (n=80 neurons from 4 HC lines and 4 SCZ lines, each line with 10 neurons).

G. Scheme of cIN organoid synapse analysis with or without activated microglia-conditioned media.

H. Analyses of inhibitory synapses in cIN organoids with or without treatment with activated microglia-conditioned media using Imaris software. The data are presented as the number of inhibitory synapses (juxtaposed GFP^+VGAT^+ puncta and $Gephyrin^+$ puncta) per 100 μm^2 of $GAD1^+$ cINs. Scale bar= 5 μm. Data are presented as mean ±SEM (n = 30 116 μm x 116 μm images per group). Two-Level Hierarchical Linear Mixed Effect Model after log-transformation was used for analysis.

The lines used in these experiments are summarized in Supplementary Table 10.

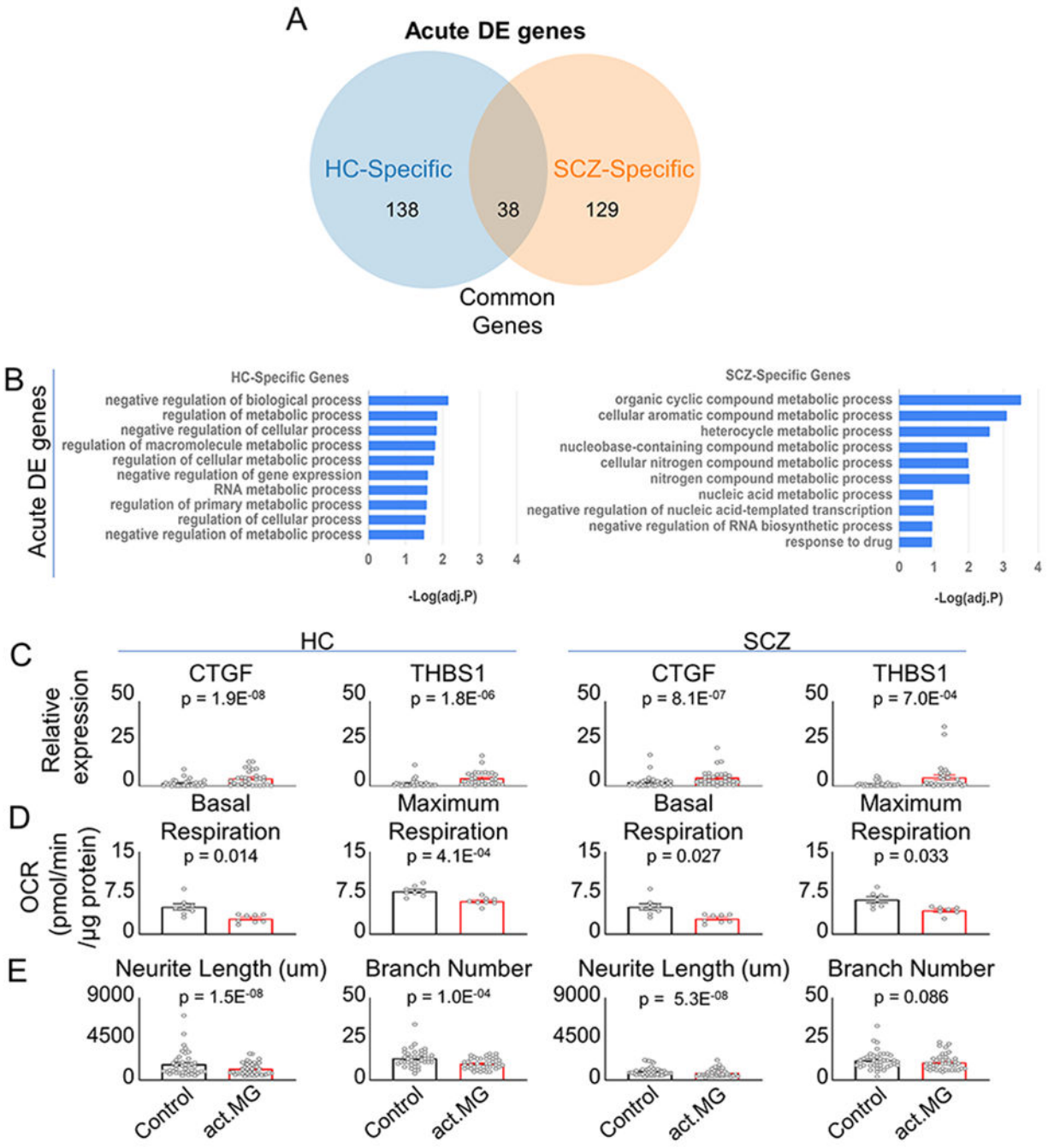

Fig. 3. Both HC cINs and SCZ cINs show metabolic dysfunction with activated microglia co-culture.

A. Venn diagram of acute phase DE genes with or without activated microglia co-culture in HC cINs and SCZ cINs.

B. Pathway analysis of acute phase DE genes with or without activated microglia co-culture in HC cINs and SCZ cINs using DAVID (https://david.ncifcrf.gov/summary.jsp). Significant enrichment was tested by the Fisher's Exact Test.

C. qPCR analysis of *CTGF* and *THBS1* expression with or without activated microglia coculture in HC cINs or SCZ cINs. Data were normalized by *GAPDH* expression and are

presented as mean±SEM. Two-Level Hierarchical Linear Mixed Effect Model after log-transformation was used for analysis (n=30 batches from 10 lines, each line with 3 independent differentiations).

D. Analysis of oxidative phosphorylation using a Seahorse Analyzer, showing significant decreases in mitochondrial function in cINs cultured in activated microglia-conditioned media both in HC cINs and SCZ cINs. Data are presented as mean±SEM. Two-tailed paired t-test was used for analysis (n=8 lines for HC and n=7 lines for SCZ, Basal Respiration of HC: t=3.248, df=7, Maximum Respiration of HC: t=6.266, df=7, Basal Respiration of SCZ: t=2.884, df=6, Maximum Respiration of SCZ: t=2.744, df=6).

E. Arborization analysis of HC cINs or SCZ cINs infected with a limiting titer of GFP-expressing lentivirus and cultured with or without activated microglia-conditioned media. Images were analyzed using ImageJ with the Neuron J plugin. Center and error bars show mean ± SEM. Two-Level Hierarchical Linear Mixed Effect Model after log-transformation was used for analysis of Neurite Length and Two-Level Hierarchical Mixed Effect Log-Linear Model was used for analysis of Branch Number (n=40 neurons for 4 HC lines and n=40 neurons for 4 SCZ lines, each line with 10 neurons).

The lines used in these experiments are summarized in Supplementary Table 10.

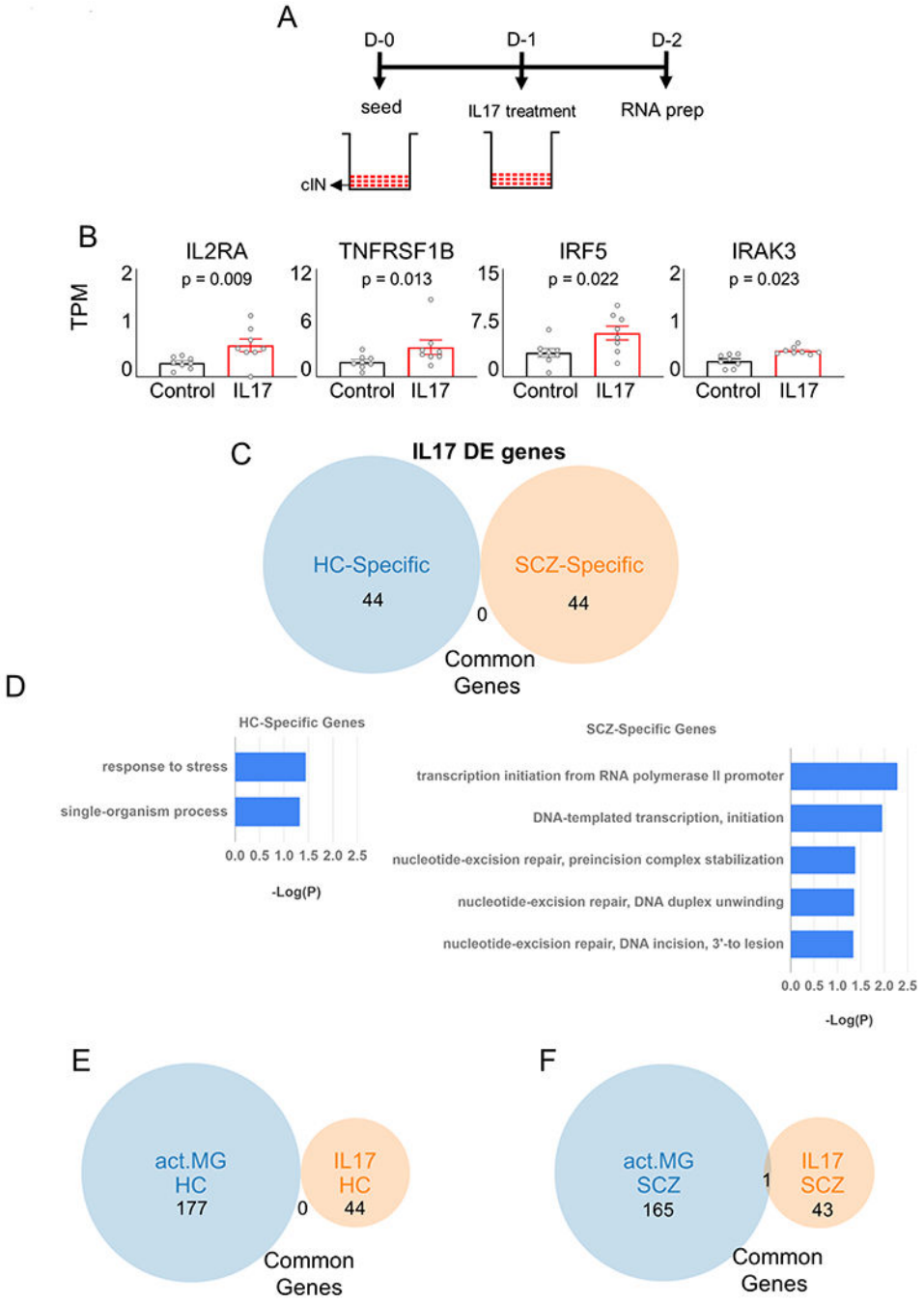

Fig. 4. Neither HC nor SCZ cINs show metabolic dysfunction under IL17 treatment.

A. Scheme for treating cINs with IL17.

B. RNA-seq analysis of cINs with or without IL17 treatment. Gene expression is shown as TPM, obtained from Kallisto. Differentially expressed genes were analyzed by DESeq2 (Wald test for two-sided significance testing, n=8 independent differentiations from 4 HC lines and 4 SCZ lines). Error bars are SEM.

C. Venn diagram of DE genes with or without IL17 treatment in HC cINs and SCZ cINs.

D. Pathway analysis of DE genes with or without IL17 treatment in HC cINs and SCZ cINs using DAVID (https://david.ncifcrf.gov/summary.jsp). Significant enrichment was tested by the Fisher's Exact Test.

E. Venn diagram of DE genes for activated microglia co-culture vs. IL17 treatment in HC cINs.

F. Venn diagram of DE genes for activated microglia co-culture vs. IL17 treatment in SCZ cINs.

The lines used in these experiments are summarized in Supplementary Table 10.

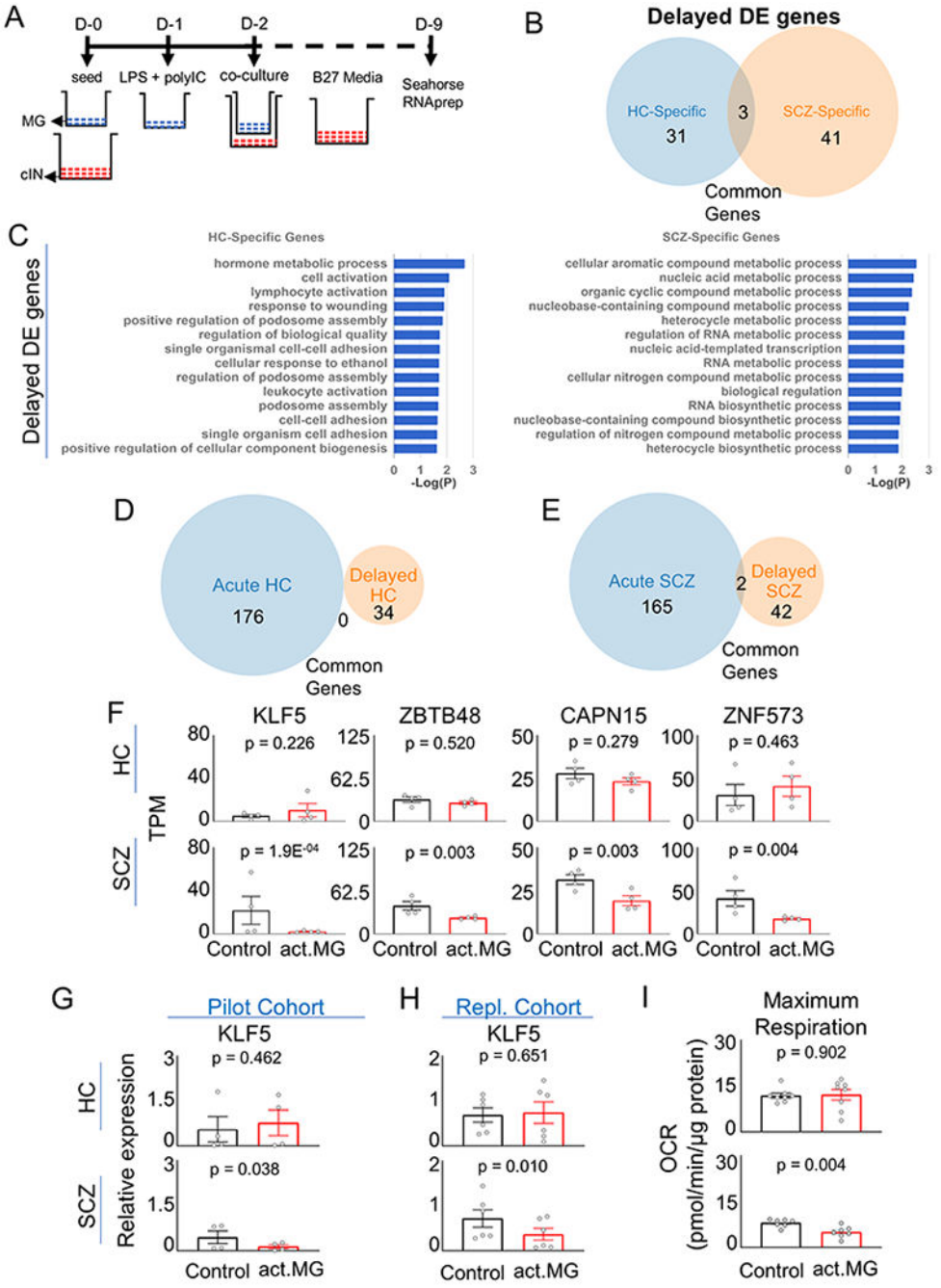

Fig. 5. SCZ cINs but not HC cINs show metabolic dysfunction even after removal of activated microglia co-culture.

A. Scheme for cell treatment to analyze prolonged effects even after removal of co-cultured activated microglia.

B. Venn diagram of DE genes with or without activated microglia co-culture in HC cINs and SCZ cINs one week after the removal of activated microglia co-culture.

C. Pathway analysis of DE genes with or without activated microglia co-culture in HC cINs and SCZ cINs one week after the removal of activated microglia co-culture using DAVID

(https://david.ncifcrf.gov/summary.jsp). Significant enrichment was tested by the Fisher's Exact Test.

D. Venn diagram of DE genes of acute phase vs. one week after removal of activated microglia co-culture in HC cINs.

E. Venn diagram of DE genes of acute phase vs. one week after removal of activated microglia co-culture in SCZ cINs.

F. RNA-seq analysis of cINs with or without activated microglia co-culture one week after removal of activated microglia co-culture. Gene expression is shown as TPM (Transcripts Per Million), obtained from Kallisto. Differentially expressed genes were analyzed by DESeq2 (Wald test for two-sided significance testing, n=8 independent differentiations from 4 HC lines and 4 SCZ lines). Error bars are SEM.

G. qPCR analysis of *KLF5* expression in cINs with or without activated microglia co-culture one week after the removal of activated microglia co-culture. Data were normalized by *GAPDH* expression and are presented as mean±SEM. Two-tailed paired t-test after log transformation was used for analysis (n=4 lines for HC and n=4 lines for SCZ; Each data point is averaged from 3 independent differentiations, HC: t=0.8405, df=3, SCZ: t=3.550, df=3).

H. qPCR analysis of *KLF5* expression in replication cohort of cINs with or without activated microglia co-culture one week after the removal of activated microglia co-culture. Data were normalized by *GAPDH* expression and are presented as mean±SEM. Two-tailed paired t-test was used for analysis (n=6 lines for HC and n=6 lines for SCZ; Each data point is averaged from 3 independent differentiations, HC: t=0.4805, df=5, SCZ: t=3.999, df=5).

I. Analysis of oxidative phosphorylation using a Seahorse Analyzer, showing significant decreases in mitochondrial function in SCZ cINs (lower panel) but not in HC cINs (upper panel) one week after removal of the activated microglia-conditioned media. Data are presented as mean±SEM. Two-tailed paired t-test was used for analysis (n=8 lines for HC and n=7 lines for SCZ; Each data point is averaged from 1-4 independent differentiations, Maximum Respiration of HC: t=0.1277, df=7, Maximum Respiration of SCZ: t=4.428, df=6).

The lines used in these experiments are summarized in Supplementary Table 10.

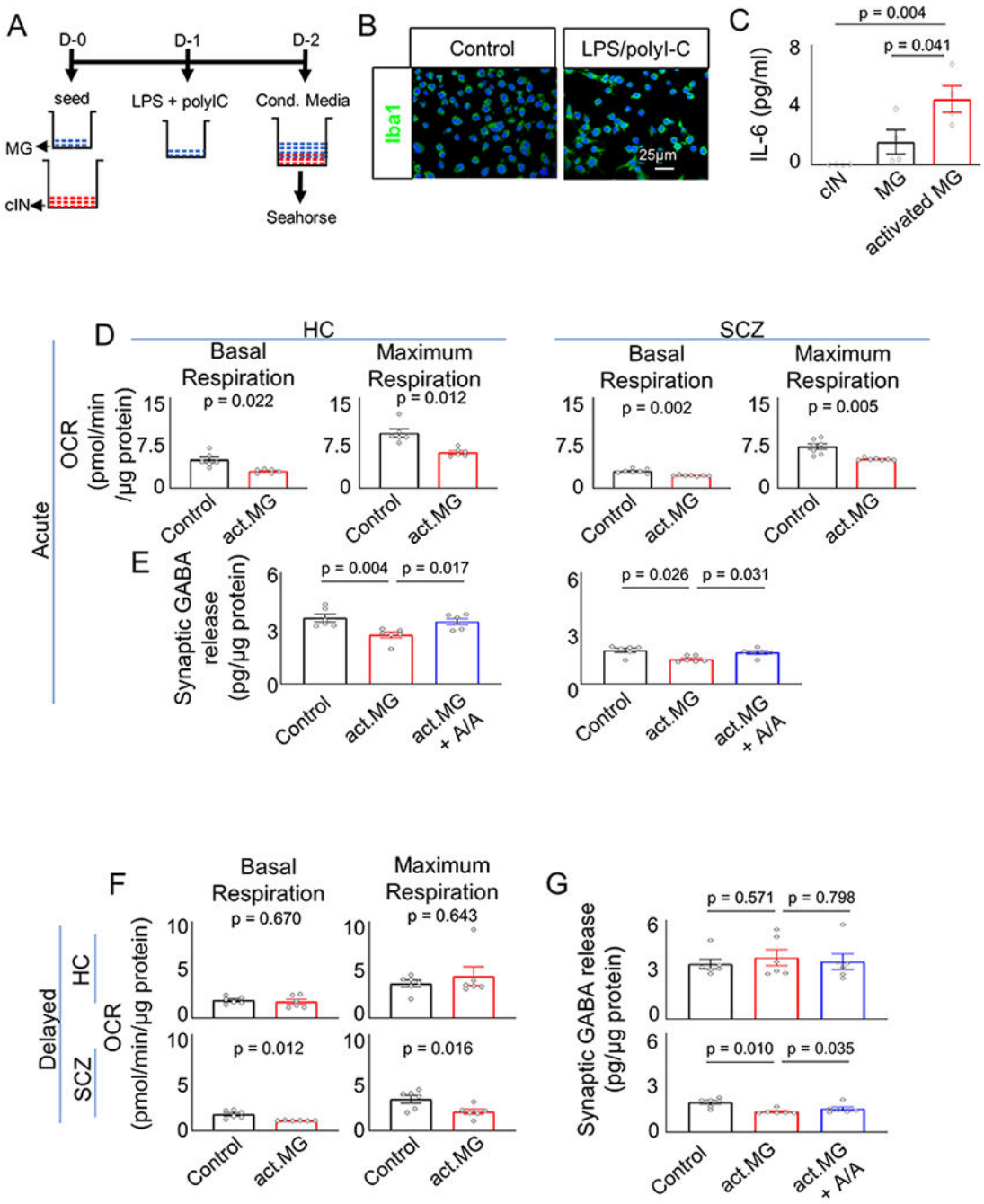

Fig. 6. cINs treated with activated HMC3-conditioned media show metabolic dysfunction.

A. Scheme for culturing developmental cINs with activated microglia-conditioned media.

B. Immunocytochemistry analysis of HMC3 microglia with or without activation with LPS and polyI-C. Scale bar= 25 μm. Analysis was repeated at least three times with comparable results.

C. ELISA analysis of human IL-6 release from activated microglia HMC3. Data are presented as mean±SEM. One-way ANOVA followed by posthoc analysis using Tukey's

multiple comparisons test was used for analysis (p=0.0048 and n=4 independent experiments, f=10.22, df=2).

D. Analysis of oxidative phosphorylation using a Seahorse Analyzer, showing significant decreases in mitochondrial function with activated microglia-conditioned media both in HC cINs and SCZ cINs. Data are presented as mean±SEM. Two-tailed paired t-test was used for analysis (n=6 lines for HC and n=7 lines for SCZ, Basal Respiration of HC: t=3.271, df=5, Maximum Respiration of HC: t=3.830, df=5, Basal Respiration of SCZ: t=5.116, df=6, Maximum Respiration of SCZ: t=4.301, df=6).

E. Action potential firing-dependent synaptic GABA release analysis of HC cINs or SCZ cINs cultured without activated HMC3 microglia-conditioned media, with activated microglia-conditioned media or with activated microglia-conditioned media + ALA/ALC treatment. Center and error bars show mean ± SEM. One-way ANOVA, followed by posthoc analysis using Dunnett's multiple comparisons test (n=6 lines for HC and n=6 lines for SCZ; Each data point is averaged from 1-3 independent differentiations, HC: f=9.228, df=2, SCZ: f=6.138, df=2).

F. Analysis of oxidative phosphorylation using a Seahorse Analyzer, showing significant decreases in mitochondrial function in SCZ cINs but not in HC cINs one week after removal of activated HMC3 microglia-conditioned media. Data are presented as mean±SEM. Two-tailed paired t-test was used for analysis of HC Basal Respiration and Two-tailed paired t-test after log transformation was used for analysis of HC Maximum Respiration. Two-tailed paired t-test was used for analysis of SCZ Basal Respiration and SCZ Maximum Respiration (n=6 lines for HC and n=6 lines for SCZ, Each data point is averaged from 1-4 independent differentiations, Basal Respiration of HC: t=0.4513, df=5, Maximum Respiration of HC: t=0.4917, df=5, Basal Respiration of SCZ: t=3.784, df=5, Maximum Respiration of SCZ: t=3.566, df=5).

G. Analysis of Action potential firing-dependent synaptic GABA release analysis of HC cINs or SCZ cINs cultured without activated HMC3 microglia-conditioned media, with activated microglia-conditioned media or with activated microglia-conditioned media + ALA/ALC treatment. Data are presented as mean±SEM. One-way ANOVA, followed by posthoc analysis using Dunnett's multiple comparisons test (n=6 lines for HC and n=6 lines for SCZ; Each data point is averaged from 1-3 independent differentiations, HC: f=0.6048, df=2, SCZ: f=12.82, df=2).

The lines used in these experiments are summarized in Supplementary Table 10.

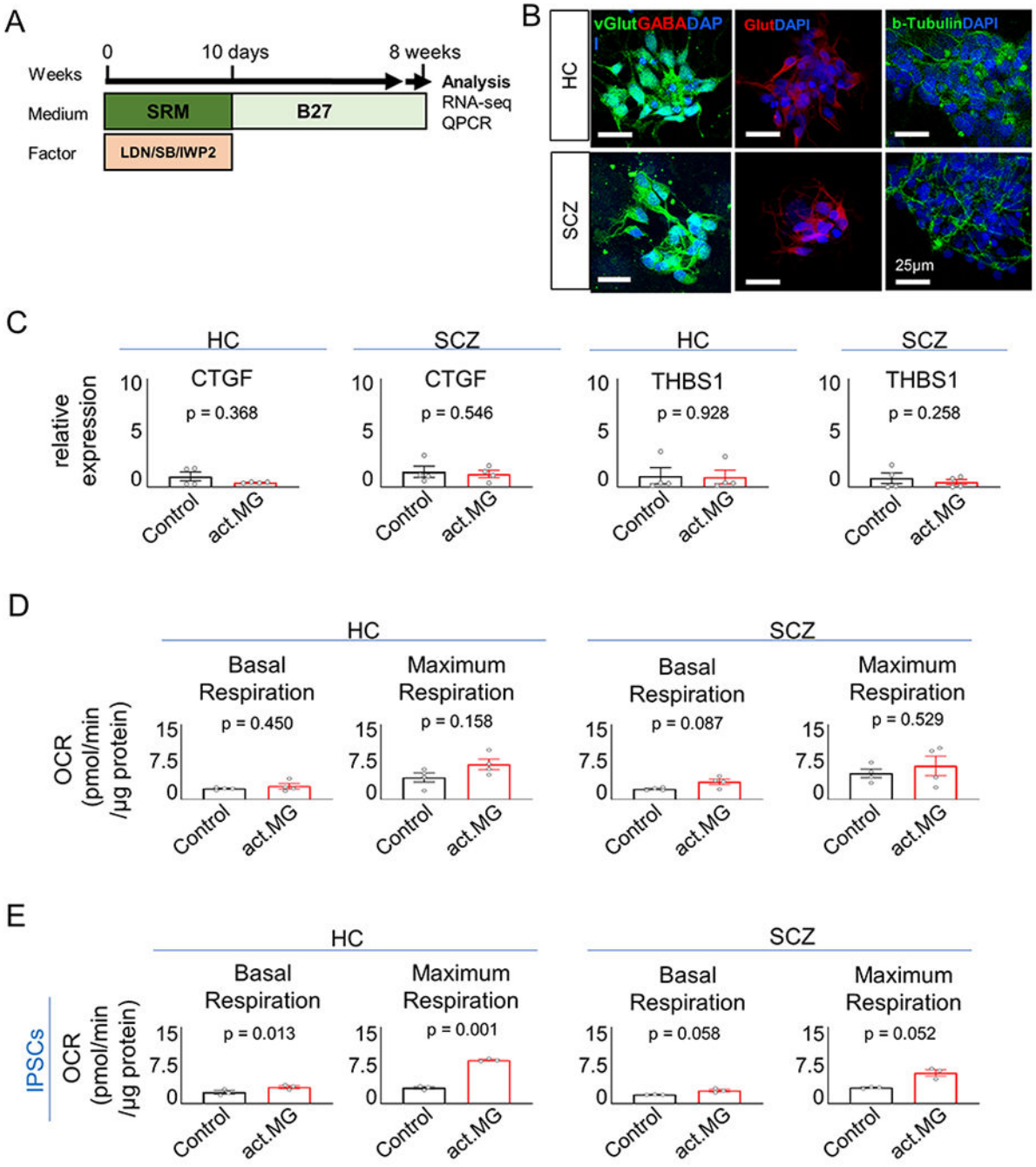

Fig. 7. Neither developmental glutamatergic neurons nor SCZ iPSCs cultured in activated microglia-conditioned media show metabolic dysfunction.

A. Scheme for generating developmental glutamatergic neurons.

B. Immunocytochemistry analysis of differentiated glutamatergic neurons from HC vs SCZ iPSCs. Scale bar= 25 μm. Analysis was repeated at least three times with comparable results.

C. qPCR analysis of *CTGF* and *THBS1* expression with or without activated HMC3 microglia-conditioned media in HC glutamatergic neurons or SCZ glutamatergic neurons. Data were normalized by *GAPDH* expression and are presented as mean±SEM. Two-Level Hierarchical Linear Mixed Effect Model after log-transformation was used for analysis of

HC *CTGF* and *THBS1* and Two-Level Hierarchical Linear Mixed Effect Model was used for analysis of SCZ *CTGF* and *THBS1* (n=4 batches from 2 lines, each line with 2 independent differentiations).

D. Analysis of oxidative phosphorylation using a Seahorse Analyzer, showing no changes in mitochondrial function either in HC glutamatergic neurons or SCZ glutamatergic neurons cultured in activated HMC3 microglia-conditioned media. Data are presented as mean ±SEM. Two-Level Hierarchical Linear Mixed Effect Model after log transformation was used for analysis of HC Basal Respiration and Two-Level Hierarchical Linear Mixed Effect Model was used for analysis of HC Maximum Respiration, SCZ Basal Respiration and SCZ Maximum Respiration (n=4 batches from 2 lines, each line with 2 independent differentiations).

E. Analysis of oxidative phosphorylation in iPSCs using a Seahorse Analyzer. Data are presented as mean±SEM. Two-tailed paired t-test was used for analysis (n=3 batches from 1 line for HC and n=3 batches from 1 line for SCZ, Basal Respiration of HC: t=8.404, df=2, Maximum Respiration of HC: t=28.98, df=2, Basal Respiration of SCZ: t=3.960, df=2, Maximum Respiration of SCZ: t=4.190, df=2).

The lines used in these experiments are summarized in Supplementary Table 10.